Viktor Schallert, BSc

Degradation of natural rubber via cross-metathesis with electron-deficient enes and the use of the saponified products as stabilizers for high internal phase emulsions

MASTER'S THESIS

to achieve the university degree of

Diplom-Ingenieur

Master's degree programme: Technical Chemistry

submitted to

Graz University of Technology

Supervisor

Assoc.Prof. Dipl.-Ing. Dr.techn. Christian Slugovc

Institute for Chemistry and Technology of Materials

Graz, October 2019

AFFIDAVIT

I declare that I have authored this thesis independently, that I have not used other than the declared sources/resources, and that I have explicitly indicated all material which has been quoted either literally or by content from the sources used. The text document uploaded to TUGRAZonline is identical to the present master's thesis.

Date

Signature

Wer will was Lebendiges erkennen und beschreiben,
sucht erst den Geist herauszutreiben,
dann hat er die Teile in seiner Hand,
fehlt, leider, nur das geistige Band.

Johann Wolfgang von Goethe

Acknowledgement

First and foremost, I would like to thank Prof. Christian Slugovc for his extensive help during the whole cause of my research and for the opportunity to work in his research group.

I'd also like to express my gratitude to the staff of ICTM for conducting analysis and giving support during interpretation. Namely, I want to thank Prof. Robert Saf for taking the SEM images, Karin Bartl for measuring the MALDI-TOF spectra and Josefine Hobisch for measuring the SEC spectra.

Furthermore, I'd like to thank Efthymia Vakalopoulou for her advice and assistance concerning HIPE formation, polymerization and analysis.

I'd like to thank the whole working group, especially Petra Hofstadler, for their professional advice and good work environment.

And last but not least, I would especially like to thank my parents for their support which made my studies possible in the first place.

Abstract

The degradation of natural rubber goods, namely rubber gloves, via cross-metathesis with electron-deficient olefins, yielding enoate-endcapped oligoisoprenes, is studied. Based on knowledge gained in a previous work, herein the focus is put on discovering ways to reduce the catalyst amount necessary for this reaction. Emphasis is laid on using electron-deficient olefins other than previously used ethyl acrylate and on developing a pre-treatment of the rubber gloves allowing for a better accessibility of the rubber's double bonds. While fumarate and maleate derivatives as well as acrylic acid showed poor or no conversion of the rubber, methyl crotonate was identified as a possible alternative for acrylates. Moreover, it has been shown that phosphine bearing pre-catalysts are competitive to more expansive phosphine free variants. As a result, the enoate-endcapped oligoisoprene formation can be obtained in higher yield with lower amounts of a cheaper catalyst. In a second step, the obtained oligomers were saponified, yielding ionic amphiphiles which were then tested for their ability to stabilize high internal phase emulsions of water in dicyclopentadiene. The corresponding sodium salt of oligomers with about 6.5 isoprene repeating units were found to be suited for that task. Subsequently, the high internal phase emulsions were cured via ring opening metathesis polymerization and the obtained macroporous polymer foams were characterized. With that result a novel opportunity for using rubber waste derived products has been disclosed.

Table of contents

1 Introduction

In times of rapid climate change and pollution the consequent increased awareness for nature and its conservation is more prevailing than ever. In the global effort for a liveable future, also chemistry has its part. One way of improvement in these regard is the reuse of waste material. Besides the well-known term recycling there exist also down- and upcycling. While down- and recycling only give products of less or at least the same value, upcycling gives the opportunity to transform low cost waste into high price products, adding an economical dimension.

Natural rubber (*cis*-1,4-polyisoprene, NR) is a green raw material from the rubber tree, normally crosslinked via sulphide or peroxide bridges to get a wide variety of materials of daily use like rubber tires, rubber gloves, condoms, sealings, air balloons and many more. To gain reusable materials from these, sooner or later to-be waste materials, already many degradation processes are established. Namely thermo-mechanical degradation, usually including a degradation agent,[1,2] biological degradation by bacteria or funghi[3–5] and chemical degradation[6] including reversed acyclic diene metathesis with ethene.[7] As the latter leads only to the formation of shorter NR chains, the use of alternative cross-metathesis (CM) partners than ethene comes to mind. This way telechelic or semi-telechelic oligomers can be retrieved,[8] adding a higher value to the product. By extending this route to electron-deficient alkenes, the versatility of the end-groups is increased as the resulting telechelic double bond differs from those in the olefinic oligomer back bone in its electron-deficient character, making reactions like the Michael-addition or the Diels-Alder-cycloaddition possible.

One of the first things that come to mind when talking about end-group functionalized of long nonpolar chains are surfactants. These find a wide field of application from detergents over wetting agents to stabilizers. Of those, stabilizers give the opportunity to form different structures in emulsions depending on the chain length, types of attached groups and composition of the emulsion. This is called molecular templating and can give different structures like bicontinous build-ups, hexagonal tube arrangements or simple micelles. A special case of emulsion that can be formed is the so called high internal phase emulsion (HIPE). Here the maximal packing density of spheres of 74% is topped, leading to a macro-porous foam. Via consequent polymerisation of the external phase and removal of the internal one, a porous interconnected, bicontinous solids can be formed. These are capable of taking up a multitude of their own weight in solvent and on the other hand have a high surface area, making for instance the trapping of surrounding gases or hazardous liquids possible.

2 Theoretical part

2.1 Olefin metathesis

In 1964, Banks reported the disproportionation of propylene to *n*-butene and ethene in the presence of $Mo(CO)_6$, $W(CO)_6$ or Co-oxide and 'Molybdena' catalysts.[9] This was the first mentioning of catalytic olefin metathesis, a reaction where double bonds of olefins are broken and reformed, exchanging the carbon atoms at the double bonds of the two involved olefins (Figure 1).

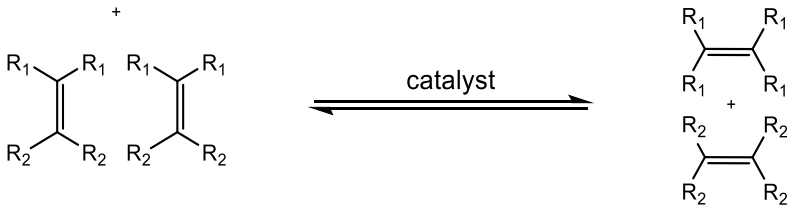

Figure 1: principal of the olefin metathesis reaction

Olefin metathesis is an equilibrium reaction that can be controlled thermodynamically.[10] In practice this allows for shifting the equilibrium by using reaction partners with no or only small rests at one carbon atom of the double bond, forming highly volatile compounds like ethylene or 2-butene. Another approach is the use of high-energy compounds such as cyclooctene, cyclobutene or norbornene in ring opening metathesis polymerisation (ROMP), where the release of the ring strain drives the reaction. By forming highly substituted products, which are strongly hindered in the back reaction, the formation of a favoured product can also be promoted.[11] It is also important to mention the formation of *cis*/*trans* isomers during olefin metathesis (Figure 2), which can be controlled sterically. This also leads to the isomerisation of educts which in turn shines a light on degenerate self-metathesis pathways where two educt molecules react in a way where neither the desired product nor side-product but two new educt molecules are formed. As the lifetime of metathesis catalysts is limited, such degenerate pathways can severely lower the effectiveness of a reaction.

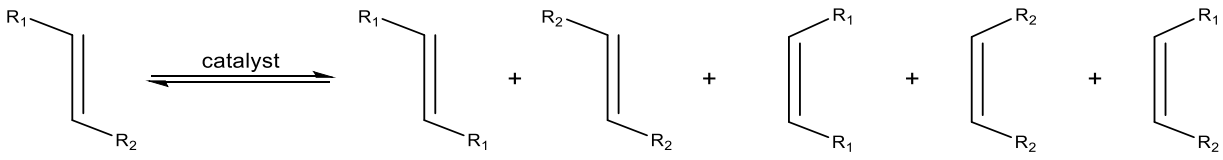

Figure 2: possible isomeric products from metathesis of a single olefinic compound

Olefin metathesis today finds wide variety of applications. The most important subtypes are CM, ring closing metathesis (RCM), ring opening metathesis (ROM), acyclic diene metathesis (ADMET) and ROMP (Figure 3).

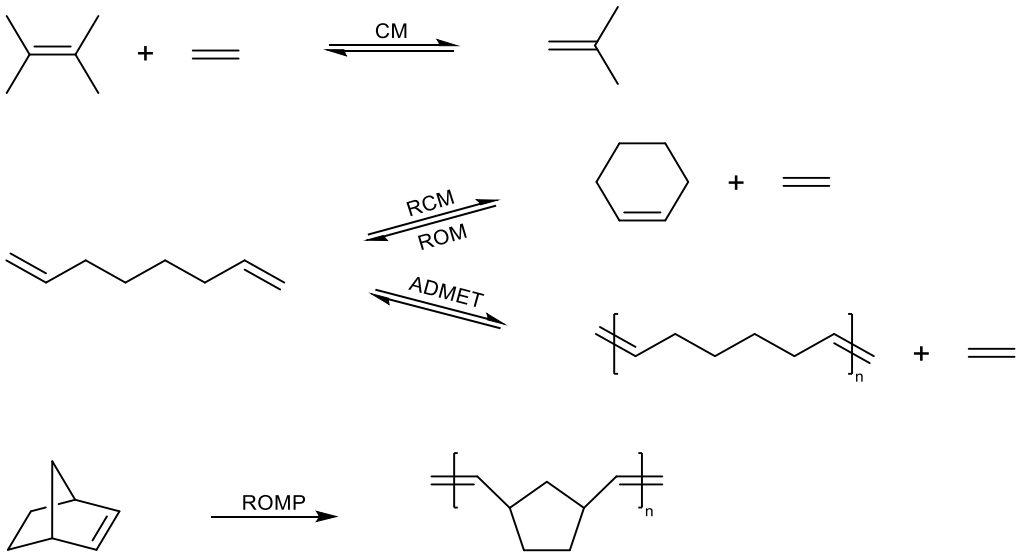

Figure 3: subtypes of olefin metathesis

In 1970, Chauvin proposed the now widely accepted mechanism for the catalytic olefin metathesis (Figure 4).[12] Here in a first step an olefin coordinates to the metal atom of the catalytic metal-alkylidene species. Then this olefin shifts to form a metallocyclobutane (MCB) intermediate before a perpendicular shift to the first one occurs, leading to the formation of a new olefin. After this new olefin is released, a new catalytic cycle can begin. Overall, the reaction can be split into two different parts, the initiation and the propagation. While the latter represents the desired metathetic reaction with all its side-product formation and degenerate pathways, the initiation is the first cycle a catalyst molecule undergoes. This leads to the formation of usually unwanted metathesis products, containing the alkylidene unit of the original catalyst and the first catalytic metal-alkylidene species that can perform the desired reaction. Nevertheless, corresponding to the catalyst-loading, typically only small, negligible amounts of those are formed.

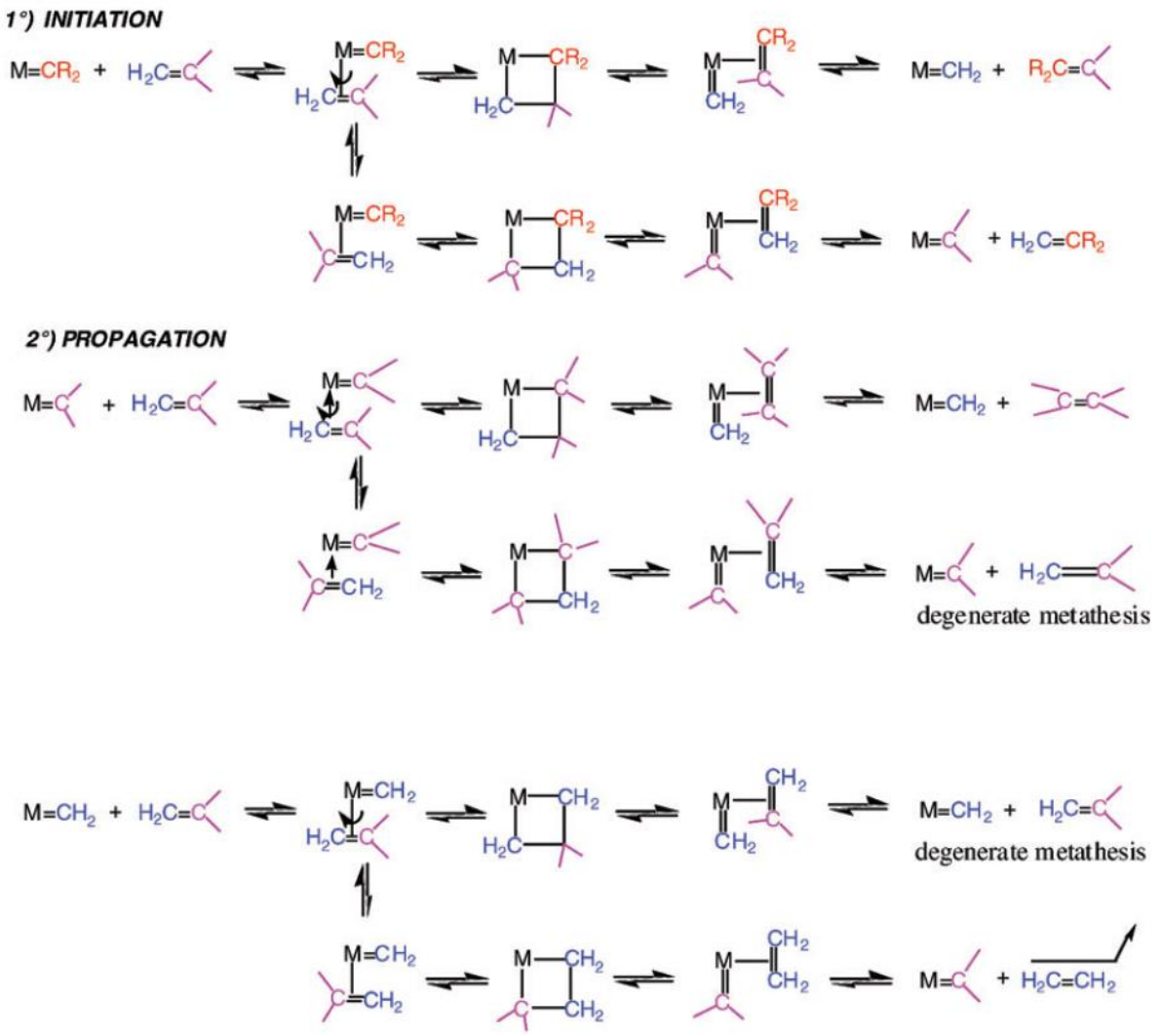

Figure 4: Chauvin mechanism of olefin metathesis[10]

Of the many different metal central atoms, capable of catalysing olefin metathesis, molybdenum, tungsten and ruthenium are the most widely spread, laying ground to highly active and selective catalysts. While in Mo- and W-based catalysts comprise a high oxidation state and ligands that increase the central atoms electrophilicity, in Ru-catalysts basic ligands are used. Those promote the detachment of a ligand, generating the active species. In general, transition-metals from higher groups show a higher affinity towards soft Lewis bases such as olefins than towards hard Lewis bases such as alcohols or acids, explaining the higher functional group tolerance of Ru-systems compared to Mo- and W-systems. Os- and Ir-systems are also known to be metathesis active, but are too expensive compared to the afore mentioned. Fe-, Co- and Rh-complexes might look metathesis active at first glance but usually lead to cyclopropanation.[13,14]

The metathesis catalysts can be classified into Schrock-,[15] Grubbs I-III[16–18] and Hoveyda-type[19] catalysts, shown in Figure 5. The Mo-based Schrock catalysts have a higher stability than similar W-based systems but have a lower storage-stability and are more sensitive towards

air, moisture and protic compounds, than the other systems. The Ru-based Grubbs systems are much more functional group tolerant and do not require as strict conditions, making them easier to handle. The introduction of N-heterocyclic carbene (NHC) ligands in Grubbs II catalysts increased activity and selectivity compared to the Grubbs I catalyst, while the switch from phosphine to pyridine ligands in Grubbs III catalysts allowed for a faster initiation. The Hoveyda systems, although initiating slower, are much more robust and can even be recycled[20] as the used chelating ligands tend to recoordinate after the metathesis reaction is finished.[13,14]

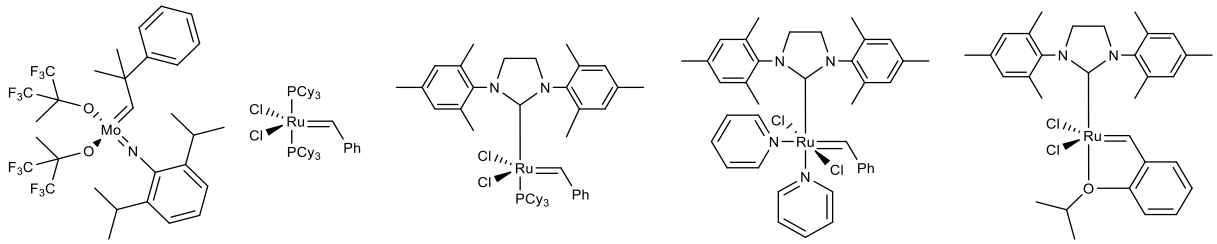

Figure 5: generations of metathesis catalysts[15-19]

2.2 Metathesis catalyst degradation due to phosphine ligands

Catalyst degradation mechanisms, that can severely influence the effectiveness of a reaction, are an ongoing challenge in olefin metathesis. Aside from the usually occurring degradation mechanisms, such as by O_2 from air or H_2O dissolved in the solvent or from the environment,[21] two degradation mechanisms, that can be traced back to the formation of a methylidene unit at the catalytic metal species under the presence of phosphine ligands, need to be mentioned here. In the herein described case, where performance issues of reactions including acrylates are tackled, these mechanisms are of special importance, as these are directly influenced by the nature of these educts as well as by the type of catalyst.

In the first case, the methylidene unit, that is formed during the standard metathesis cycle, is attacked nucleophilically by a dissociated phosphine ligand from the catalyst, giving a methylene phosphorane that is detached from the catalytic complex. The remaining catalyst-rump can than interfere with another catalyst molecule with a detached phosphine ligand. A chloride ligand from this dimer is then taken up by the methylene phosphorane, resulting in an inactive, dimeric ruthenium complex (Figure 6).[22] This decomposition can be hampered by lowering the catalyst-loading, as different species, derived from the catalyst, need to interact with each other.

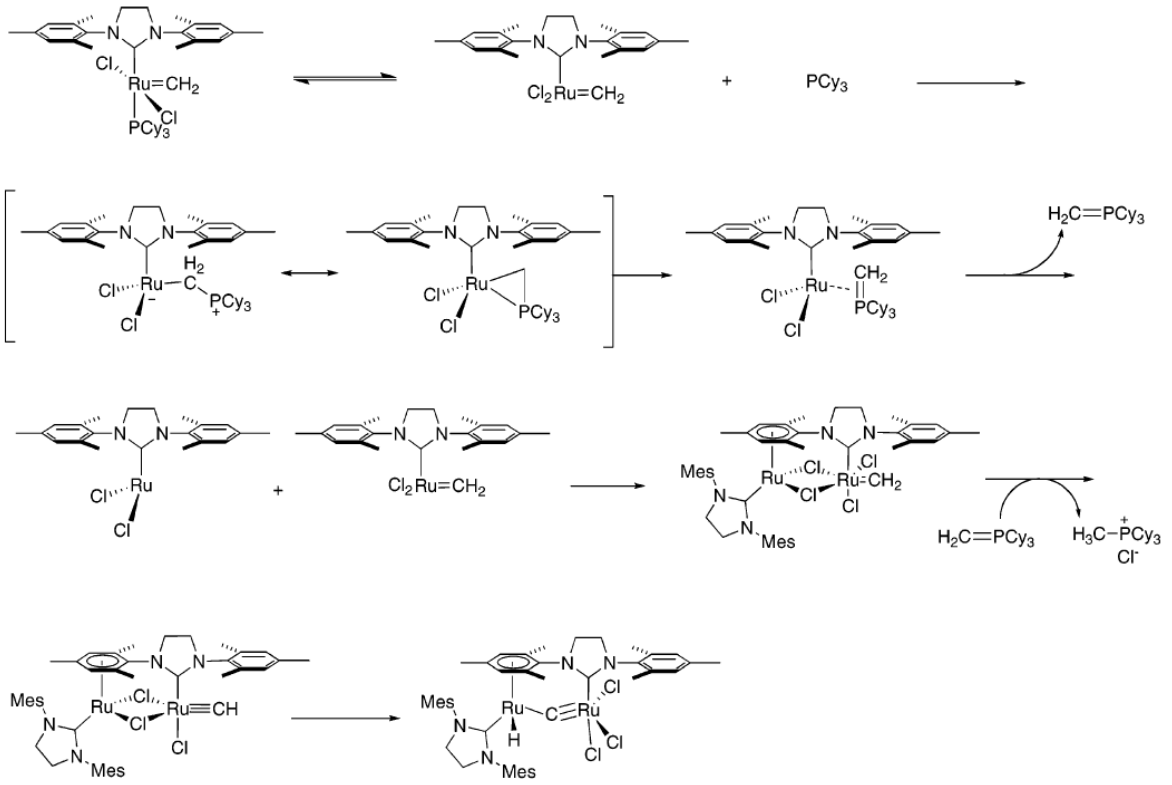

Figure 6: proposed metathesis catalyst degradation mechanism via nucleophilic attack of the phosphine ligand at the methylidene unit[22]

In the second case, a nucleophilic attack of the phosphine ligand at the double of an electron-deficient olefin occurs as shown in Figure 7. The anion of the resulting zwitterionic species (A) can then either directly attack the protons at the MCB intermediate or, more likely, attack another electron-deficient olefin. The product of this second reaction (B) then also is capable to deprotonate the MCB.[23] This decomposition can on the one hand also be prevented by lowering the catalyst-loading, as all the reactants stem from the original catalyst and need to meet up again, and on the other hand by adding acids such as phenol[24] or maleic acid[25] as the protons of these are more acidic than those of the MCB and therefore more likely to neutralize the deactivating species (A) or (B).

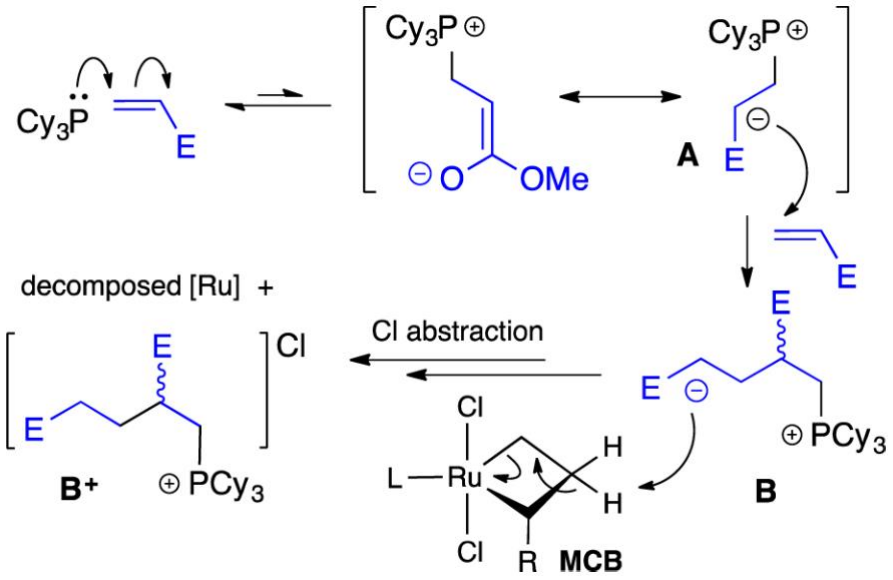

Figure 7: proposed metathesis catalyst degradation mechanism via nucleophilic attack of the phosphine ligand at the electron-deficient olefin[23]

2.3 Hydrophilic-lipophilic balance

In order to be able to make a statement about the type of emulsion an amphiphilic molecule is capable of forming, the concept of the hydrophilic-lipophilic balance (HLB) was introduced by the Atlas Powder Company in 1948[26] and scientifically published first in 1949 by Griffin.[27] The HLB-value of a certain stabilizing molecule gives information about the amount, size and strength of hydrophilic and lipophilic groups in a molecule relative to each other without giving any information about the stability of the formed emulsion. Table 1 shows the type of emulsion that is formed at different HLB-values.

Table 1: applications of surfactants depending on their HLB value[27]

Range of HLB values	Application
4-6	Water in oil emulsifier
7-9	Wetting agent
8-18	Oil in water emulsifier
13-15	Detergent
15-18	Solubilization

While the above mentioned and following works laid their emphasis on experimental determination of the HLB-value and its application, Davies introduced a system that allowed for the direct calculation of HLB-values from the molecular structure of a molecule.[28] The work

focusses on the coalescence kinetics of water/oil emulsions as the phase with the faster rate of coalescence must form the inner phase while the other one forms the outer phase. These kinetics are greatly influenced by the nature of the stabilizer at the interface. In case of oil in water emulsions, the repelling forces of charged polar groups at the droplet surface as well as the energy barrier of replacement of water on hydrated polar groups hinder the recombination of the nonpolar droplets. In contrast to this, in water in oil emulsions the penetration of the stabilizing layer by water molecules is hampered by nonpolar groups. The relatively complicated equations behind these kinetics were strongly simplified by introducing the concept of group numbers, giving different groups in the stabilizer a certain number in regard to their effect on recombination kinetics.

Table 2: HLB group numbers[28]

Hydrophilic groups	Group number
$-SO_4^-Na^+$	38.7
$-COO^-K^+$	21.1
$-COO^-Na^+$	19.1
N (tertiary amine)	9.4
Ester (sorbitan ring)	6.8
Ester (free)	2.4
-COOH	2.1
Hydroxyl (free)	1.9
-O-	1.3
Hydroxyl (sorbitan ring)	0.5
Lipophilic groups	
-CH-	-0.475
$-CH_2-$	
CH_3 -	
=CH-	
Derived groups	
$-(CH_2-CH_2-O)-$	+0.33
$-(CH_2-CH_2-CH_2-O)-$	-0.15

By inserting the group numbers, given in Table 2, of all the groups of a given amphiphilic molecule in Equation 1, the HLB-value can easily be calculated, rendering laborious experimental determinations unnecessary.

$$HLB = 7 + \sum group\ numbers \quad (1)$$

Additionally, the HLB-concept allows for a straight forward evaluation of the performance of mixtures of surfactants with different HLB-values. By simply multiplying the mole fractions and HLB-values of the different components and adding them up, the HLB-value of the mixture can be calculated according to Equation 2.[28] In a practical sense this means, that the mean chain length of the polar and nonpolar chains of a stabilizer mixture give enough information to predict its performance.

$$HLB_{mixture} = \sum_{i=0}^{n} (HLB_i * mole\ fraction_i) \quad (2)$$

2.4 The Bancroft rule

In a practical sense the HLB concept can be used to separate stabilizing from non-stabilizing parts of a mixture of different molecules with different HLB-values (e.g. polydisperse block copolymers) according to the Bancroft rule.[29] This rule states, that the continuous phase in an emulsion, is the phase the stabilizing species is more soluble in. Corresponding greatly to the HLB-value, the difference in concentration depends on the rate of transfer between the two phases as this rate of transfer is influenced by the same factors as the rate of recombination in an emulsion. Therefore, non-stabilizing side-products can be removed via simple extraction in cases where the stability of the emulsion makes it temporally feasible.

2.5 High internal phase emulsions

Emulsions with an internal phase content of more than 74% (the maximal packing density of solid spheres) are called HIPE. This is possible due to deformation of the spheres of ordinary emulsions into polyhedral structures. Usually, stabilizers are needed for their formation and to keep their structure over a certain time. Another approach is the use of Pickering emulsions where solid particles are used to stabilize the emulsion. HIPEs are normally formed by slowly dropping the internal phase into a vigorously stirred solution of external phase and stabilizer as depicted in Figure 8. This way the energy barrier of emulsification can be overcome more easily than by combining the constituents before stirring. An alternative pathway for this HIPE formation is the centrifugation of an ordinary emulsion and consequent removal of the excess external phase.[30] The final structure of a HIPE depends on many different factors. The most important one is the emulsifier, necessary to stabilize the HIPE. It determines not only the type of emulsion (oil in water or water in oil) according to its HLB-value but also its stability and

therefore uniformity and droplet-size over time. This droplet-size dispersity is also affected by rate and time of stirring during HIPE formation as well as by the viscosity of the system.[30,31]

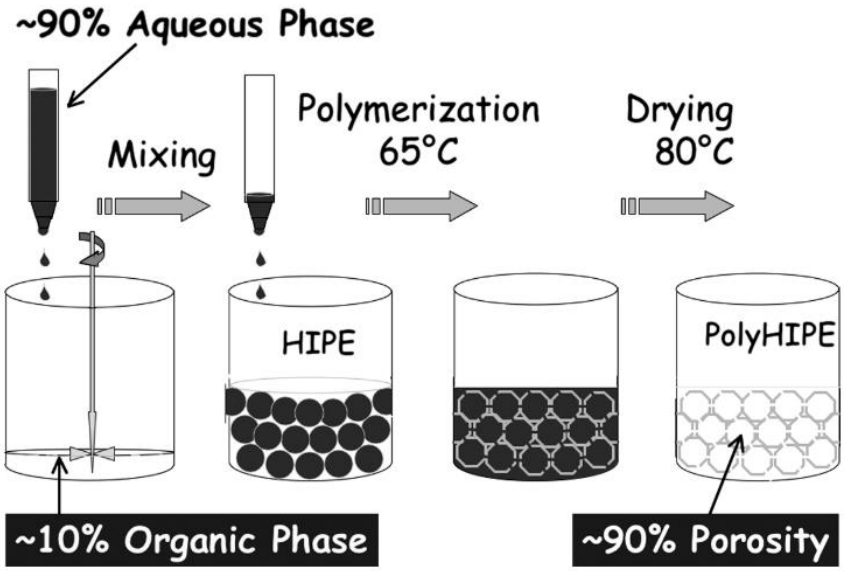

Figure 8: scheme of HIPE and polyHIPE formation[30]

The structure of HIPEs can be solidified via polymerization giving so called polymerized HIPEs (polyHIPEs) as can be seen in Figure 8. Aside from this polymer templating, HIPEs find also application in cleaning of oil and gas wells from wax and sulphur,[32] in transport of bulk-solids by pumping[33] and in cleaning of pipe systems by flushing.[34] Due to their non-Newtonian, thixotropic character, they can also be used for crowd control.[35]

2.6 Stability of HIPEs

In order to solidify the structure of a HIPE, the continuous phase is polymerised, obtaining a polyHIPE. As this polymerisation takes time and is normally performed at elevated temperatures, which also increases the speed of phase separation, hence the HIPE needs to be stable for long enough to freeze the structure. The speed of recombination of the inner phase therefore needs to be as slow as possible. In terms of stabilizer design this can be achieved by using long chains respectively strong groups in the HLB-concept, as these have a higher energetical barrier to recombination and therefore lead to a lower rate of inter-phase transfer according to the Arrhenius equation. Additionally, the stabilizer should have a structure that allows for dense packing at the interphase. In case of ionic emulsifiers, this can also be achieved by adding salts which not only increases the packing,[36] but also the polarity of the polar phase as well as the repelling forces at the surface[30,37] impeding Ostwald ripening. Overall, the higher the difference in polarity of the two phases, the more stable is the emulsion as the resulting high interfacial tension is lowered by the emulsifier, making the formation of a stabilizing film more favourable.[38] Another aspect is the viscosity of the HIPE, as an increased

viscosity decreases the rate of coalescence. However, this also affects the structure of the HIPE due to less efficient stirring, leading to a higher degree of polydispersity.[39]

2.7 polyHIPEs

The morphology of a polyHIPE, obtained by curing the external, monomer-containing phase of a HIPE, can significantly differ from that of the HIPE it originates from.[30] Two of the most important characteristics of these polyHIPEs are the sizes of the voids left behind after removal of the internal phase and of the windows forming between these voids after solidification as shown in Figure 9.

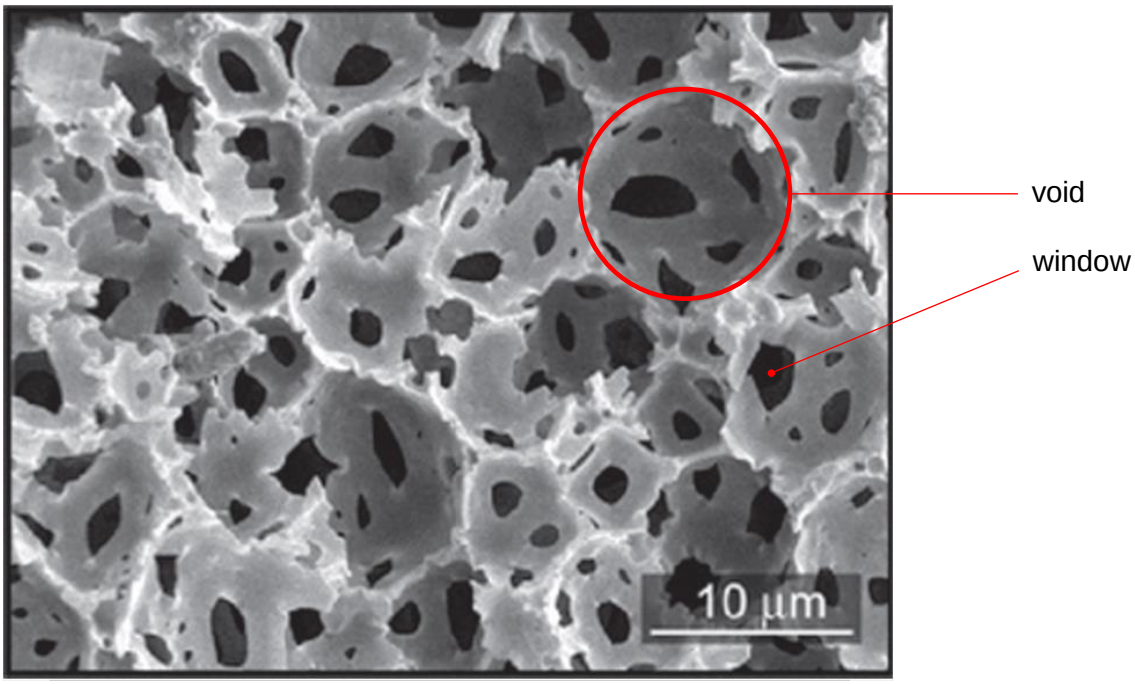

Figure 9: open cell polyHIPE structure with voids and windows[40]

The diameter of the voids, normally varying between 1 µm and 100 µm, is mainly affected by the stability of the emulsion as a decrease in stability leads to the formation of bigger voids due to Ostwald ripening during solidification.[30,31] In contrast to this, the window size depends on the thickness of the continuous phase. The thinner these walls, the more likely is the formation of windows. Therefore, the amount of external phase, but even more importantly the amount of stabilizer used, determine if an open- or closed-cell structure is formed.[30,31] In general, an open-cell structure is formed with stabilizer contents above 7% of the external phase,[41] while a stabilizer content of under 4% as well as above 80% leads to closed-cell strures.[30] This way bicontinous (solid/gaseous), highly porous monoliths with surface areas ranging from 5 to 20 m^2/g can be obtained.[30]

Their capability to absorb and pump liquids, driven by the interfacial tension between the liquid and the polyHIPE material, gives way for many applications. The scope of these applications

can be increased significantly by post-polymerisation functionalization. PolyHIPEs have already been used as chromatographic column material, support materials, transport carriers for liquids, matrices for the immobilization of cells and enzymes, for the production of living scaffolds, cleaning of water, ion exchange, in tissue engineering and hydrogen storage.[30,31,40] Due to their relatively high surface area they are also utilized as sensor material and electrode carrier material.[30,31] Additionally, polyHIPEs are used as predecessor and templates for highly porous inorganic structures that are formed via pyrolysis or calcination.[30]

3 Results and discussion

3.1 Objective

In a previous publication the metathetic degradation of NR-snippets, using ethyl acrylate as CM partner, was reported.[42] This led to the formation of semi-telechelic polyisoprene oligomers with a catalyst-loading dependent chain length, bearing enoate end-groups (Figure 10).

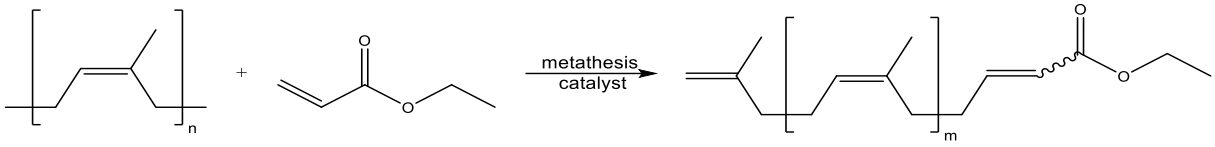

Figure 10: reported degradation of polyisoprene via CM with ethyl acrylate[42]

However, this degradation was performed using a Hoveyda-type catalyst to prevent the catalyst degradation mechanisms described in chapter 2.2. Additionally, a catalyst-loading of at least 0.5 mol% was necessary to get reproducible chain lengths.

In order to lower the catalyst-loading and make a switch to a less expensive, phosphine bearing catalyst possible, this reaction is investigated further using different electron-deficient olefins. In a second part, the saponification of the enoates is studied and the potential to use the resulting amphiphiles as stabilizers for water in oil HIPEs is targeted.

3.2 Degradation of NR-snippets via cross-metathesis with electron-deficient enes

CM of polyisoprene with other reaction partners is a challenging task due to the high degree of substitution at the double bond. In the case of electron-deficient CM-partners it becomes even harder to successfully perform this reaction, as electron-deficient enes have a lower tendency to coordinate to the metal centre of the catalytic complex and have at least one electron-withdrawing group attached, increasing the steric bulk. Nevertheless, this degradation introduces an electron-deficient end-group double bond in the otherwise electron-rich main chain, adding an additional functionality.

While the first CM attempts with ethyl acrylate give yields and chain lengths comparable to literature,[42] newly introduced alternative electron-deficient CM partners, namely dimethyl maleate, dimethyl fumarate, maleic acid, acrylic acid and methyl crotonate, show no product formation at all when using polyisoprene-snippets as substrate. Therefore, a way to improve the reaction performance overall is searched.

3.3 Pre-degradation of natural rubber

A first attempt of lowering the excess of CM partner from 5 eq. down to 2, 1 and 0.5 eq., with the intention to lower self-metathesis, gives only diminished yields but no improved performance. Therefore, another approach of making the substrate soluble is investigated. As a huge drawback of using NR-snippets is the bad accessibility of the material as the substrate can only be attacked at the surface. The effectiveness of the reaction can be increased by swelling the snippets for some time and degrading side reactions and the ongoing productive degradation increases the surface area available for the reaction over time. Nevertheless, the accessibility is still hampered compared to a solution and therefore competing side-reactions may prevail. As catalysts have a limited lifetime, these non-productive side-reactions deteriorate the reactions performance, making higher catalyst-loadings necessary. In order to overcome these challenges, a pre-degradation step is herein introduced, giving a dissolved substrate.

Metathesis is one way to degrade the NR.[8] By adding Grubbs 2nd generation type catalyst **M2** at a loading of 0.2 mol%, only incomplete degradation can be observed after holding the reaction at 80°C for 24 h. Therefore, Hoveyda type catalyst **M51** is added at a loading of 0.2 mol% and the reaction temperature is increased to 110°C. After another 24 h the NR-snippets are mostly dissolved. SEC analysis (THF, relative to poly(styrene) standards) of the product shows two hugely different signals with M_n-values of 14800 g/mol (PDI = 1.9) and 500 g/mol (PDI = 1.97). According to literature, the degradation product consists of cyclic oligoisoprene derivatives.[8] Nevertheless, this pre-degradation increases the overall need for catalyst, rendering the targeted lowering of the catalyst-loading in the CM a farce.

During an investigation on non-metathetic side reactions of dimethyl maleate with NR-snippets, a mixture of both in toluene as well as a blank, leaving out the dimethyl maleate, are left in the drying cabinet at 80°C. After one week, a clear solution without any NR-snippets is observed in both cases. No evidence of a reaction between polyisoprene and dimethyl maleate can be found, but in both cases SEC shows a dissolved polymeric material, indicating a thermal degradation of the NR-snippets. Therefore, this straight forward routine of thermal degradation is investigated further, as this pathway does not lead to contamination with other chemicals and does not make inert conditions necessary. As S-S and O-O bonds are weaker than C-C bonds the crosslinking is revoked during this thermal treatment while the polyisoprene chain is mainly broken at the bonds in β-position to the double bonds which are known to be weaker than α-C-C bonds.[43]

By increasing the temperature from 80°C to 110°C and introducing mechanical stirring, the reaction time can be decreased from one week down to 48 h. Figure 11 shows the different stages of the finally used thermal treatment. After immersion (**1**), a mechanical stirrer is used

to stir the mixture while heating, introducing additional, mechanical force for the disruption of the NR-snippets as well as allowing for a denser packing of the immersed snippets that would otherwise be non-stirrable. Following the treatment, an emulsion, already containing mostly dissolved polyisoprene, can be observed (**2**). The floating particles can be attributed to additive particles in the gloves, which are removed via centrifugation and consequent filtration. The yield of the resulting stock solution (**3**) of 77.8%, given relative to the total amount of used snippets, is relatively low for such a basic treatment. Although slight mass losses need to be expected due to the removal of the additives in the sludge after centrifugation, the main part is lost during the filtration step as here the used filter paper gets clogged by polyisoprene repeatedly and has to be changed several times. This filtration step is introduced due to a remaining slight turbidity after centrifugation and does not justify the high loss of product, but as at this time already enough dissolvable polyisoprene for the CM is prepared, no pre-degradation without filtration is performed. Investigating the molar mass of degradation product with SEC (THF, relative to poly(styrene) standards) reveals a M_n-value of 1300 g/mol (PDI = 2.2).

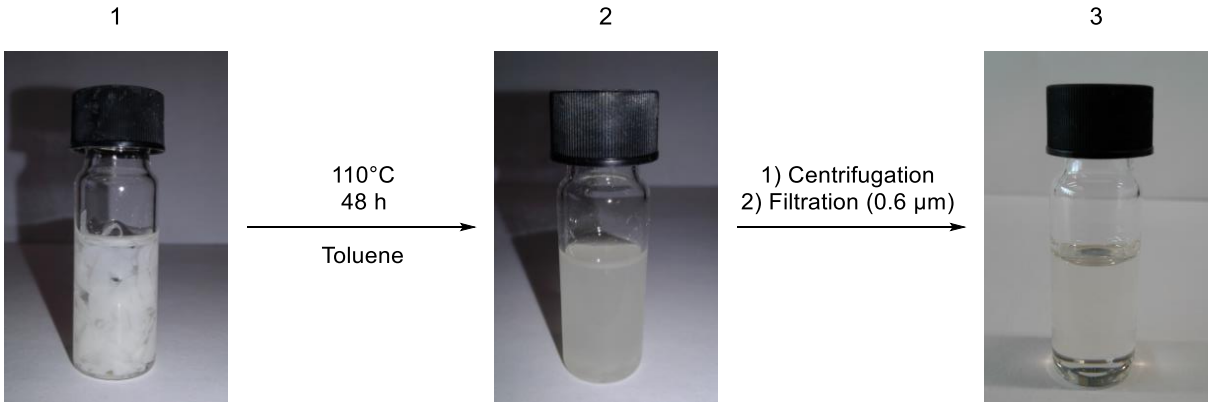

Figure 11: thermal pre-degradation of NR

3.4 Degradation of pre-degraded natural rubber via cross-metathesis with electron-deficient enes

By using pre-degraded NR, it is possible to lower the chain length of the CM product by approximately half while the yield stays constant as a comparison using ethyl acrylate shows. Degrading the NR-snippets directly gives a mean chain length of 2.7 in contrast to 1.4 in the case of pre-degraded NR. Therefore, from here on, only thermally pre-degraded polyisoprene is used. The mean chain length is determined by comparing the integrals of the peaks of the electron-deficient end-group at 5.83 to those of the isoprene repeating unit at 5.30-5.00 in the product's ^{1}H-NMR spectrum (Figure 12).

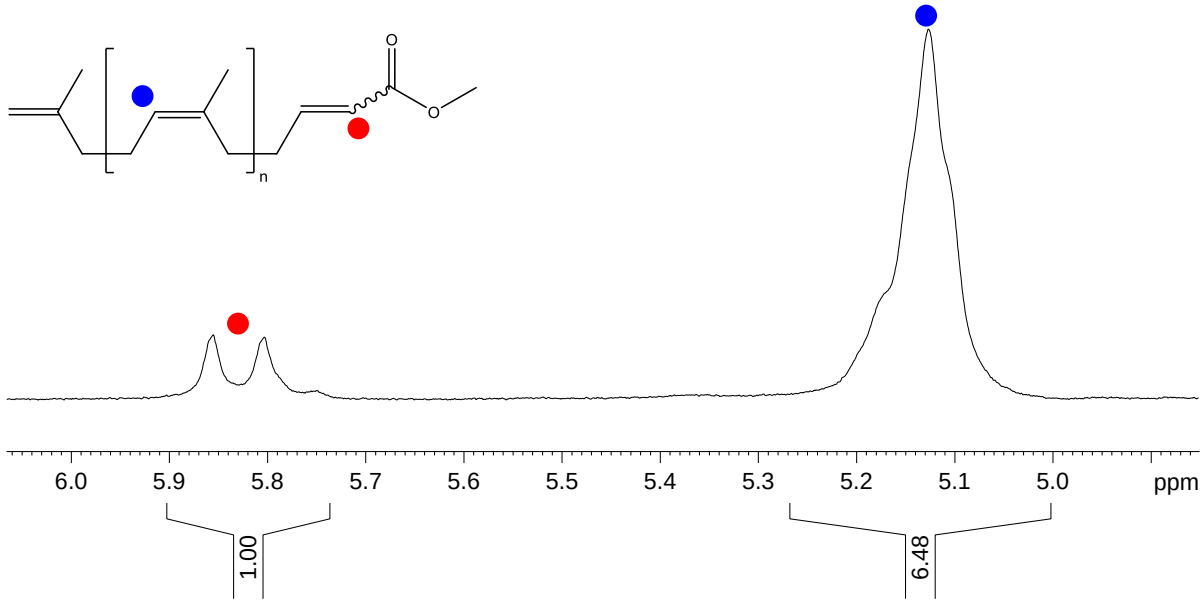

Figure 12: chain length determination (^{1}H-NMR of product from chapter 4.8)

3.4.1 Screening of alternative electron-deficient reactants

In order to find a more suitable alternative to the previously reported ethyl acrylate CM partner,[42] different compounds are tested, using the phosphine-free Hoveyda-type catalyst **M51**. Those compounds are selected according to their ability to prevent the catalyst degradation mechanisms described in chapter 2.2, to make a targeted, lower catalyst-loading of 0.1 mol% possible. Namely dimethyl maleate (**1**), dimethyl fumarate (**2**), maleic acid (**3**), acrylic acid (**4**) and methyl crotonate (**5**), shown in Figure 13, are chosen. Additionally, methyl acrylate (**6**) and ethyl acrylate (**7**) are used to produce benchmark data.

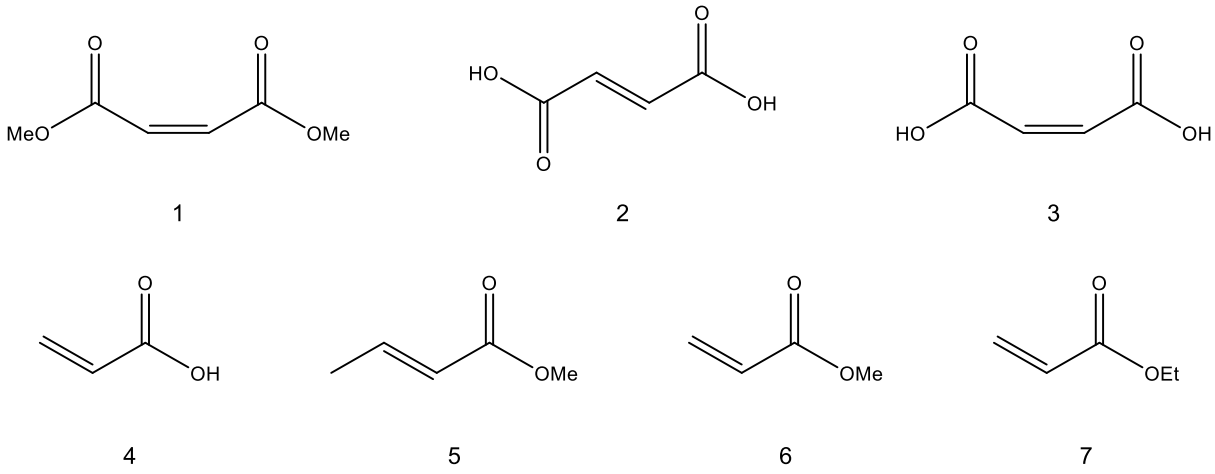

Figure 13: alternative- and benchmark-reactants for the investigated CM

Dimethyl maleate (**1**) and dimethyl fumarate (**2**) are chosen because they do not produce a methylidene unit during the metathesis cycle and would also allow for the formation of a

difunctionalized, yet telechelic, oligomeric product. But with these reactants no product formation is observed. Therefore, the less bulky maleic acid (**3**) is tested. Aside from the fact, that also in this case no CM product can be found, more polar solvents, that are still capable of dissolving the catalyst, need to be used. Overall, the unsuccessfulness of these first attempts, depicted in Figure 14, can be attributed to mechanistic reasons, which do not allow for the formation of difunctionalized oligomers (see chapter 3.5), as well as to the greatly increased electron-deficient character of double bonds containing two electron withdrawing groups, making the coordination to the metal in the catalytic metathesis cycle less likely.

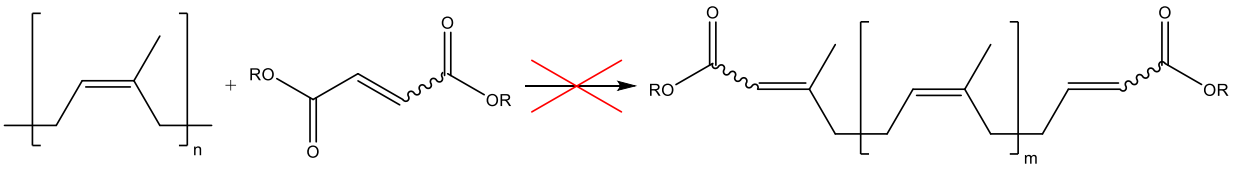

Figure 14: unsuccessful CM degradation with maleates and fumarates

Acrylic acid (**4**) is chosen due to its similarity to ethyl acrylate while in contrast to esters the acid group can impede the phospha-Michael degradation mechanism. Nevertheless, this reaction performs very poorly. While at least some minor product formation can be observed, its chain length is way above 25 and therefore practically inseparable from the nonpolar product. Additionally, polyesters, shown in Figure 15, are formed as a side-product from oxa-Michael-additions, making work-up even more difficult and leading to oligomers, functionalized with these polyesters.

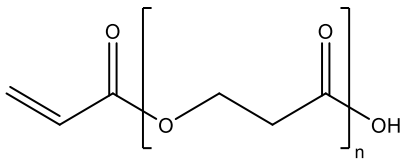

Figure 15: oxa-Michael-addition side-product (polyester)

Methyl crotonate (**5**) lacks the methylidene unit of acrylates while simultaneously not increasing the steric bulk substantially and additionally containing an electron-donating CH_3 group. It is the first reactant that gives product in reasonable yield (55.5%) and chain length (5.1) at a catalyst-loading of 0.5 mol% while at the same time not showing any formation of dimethyl fumarate as side-product.

3.4.2 Lowering of catalyst-loading

For the lowering of the catalyst-loading, additionally to the up until here used Hoveyda-type catalyst **M51**, the Grubbs 2nd generation-type catalyst **M2**, bearing a phosphine ligand, is introduced (Figure 16).

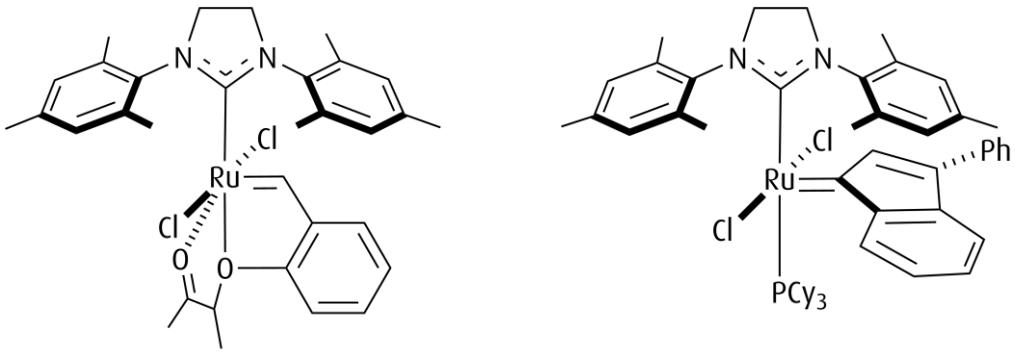

Figure 16: used metathesis catalysts (retrieved from reference 44 and 45*)*

Together with ethyl acrylate and the less bulky methyl acrylate, which was reported to give more side-product and less yield,[42] methyl crotonate is investigated using lower catalyst-loadings from 0.5 mol% down to 0.1 mol%. Lowering the catalyst-loading further to 0.05 mol% shows no product formation in any case. The overall reaction is depicted in Figure 17.

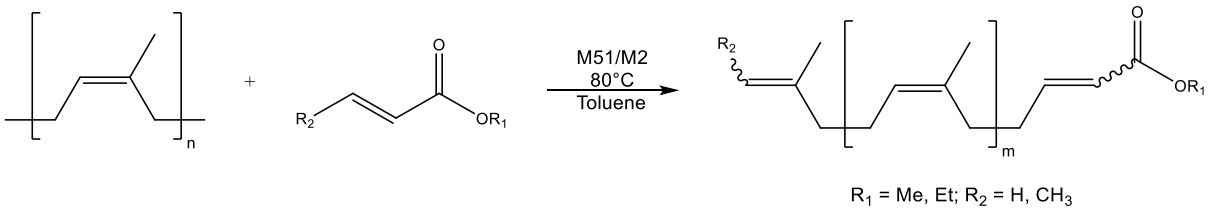

Figure 17: scheme of the degradation reaction with methyl crotonate, methyl acrylate and ethyl acrylate

Figure 18 shows the yield and resulting chain length of those reactions. The yield is calculated relative to the maximum possible amount of product that can be formed with its respective mean chain length. It can be seen, that the catalyst-loading dictates the chain length of the product oligomers, giving longer chains at lower catalyst-loadings as less productive reactions occur.

Methyl crotonate, the only alternative reactant showing product formation at a catalyst-loading of 0.5 mol%, performes very badly at lower catalyst-loadings and shows no product formation at all at the targeted catalyst-loading of 0.1 mol%. In contrast to acrylates, here the phosphine-free catalyst **M51** shows a higher activity than the phosphine-bearing **M2** and no formation of side-product (dimethyl fumarate) can be observed.

Overall, contradicting the aforementioned degradation mechanisms and the reported less efficient degradation, acrylates clearly perform best with the phosphine containing catalyst **M2**, especially at low catalyst-loadings. This can be explained by a much faster reaction speed of the productive metathesis compared to the catalyst degradation reaction as well as by the low catalyst-loading that renders the concentration dependent catalyst degradation reactions

negligible. While ethyl acrylate gives slightly lower chain lengths than methyl acrylate, the constant, much higher yield of methyl acrylate at a loading of 0.1 mol% makes this reaction more useful. In contrast to crotonate, the acrylates show formation of fumarate side-products in the range of 25 to 75% relative to the amount of product molecules. Nevertheless, these values are prone to errors as the total amounts formed are below 7 mg at catalyst-loadings below 0.5 mol%, making losses during column chromatography or while drying under vacuum significant. On the other hand, the easy removal of dimethyl fumarate during work-up gives the degradation with methyl acrylate another advantageous property.

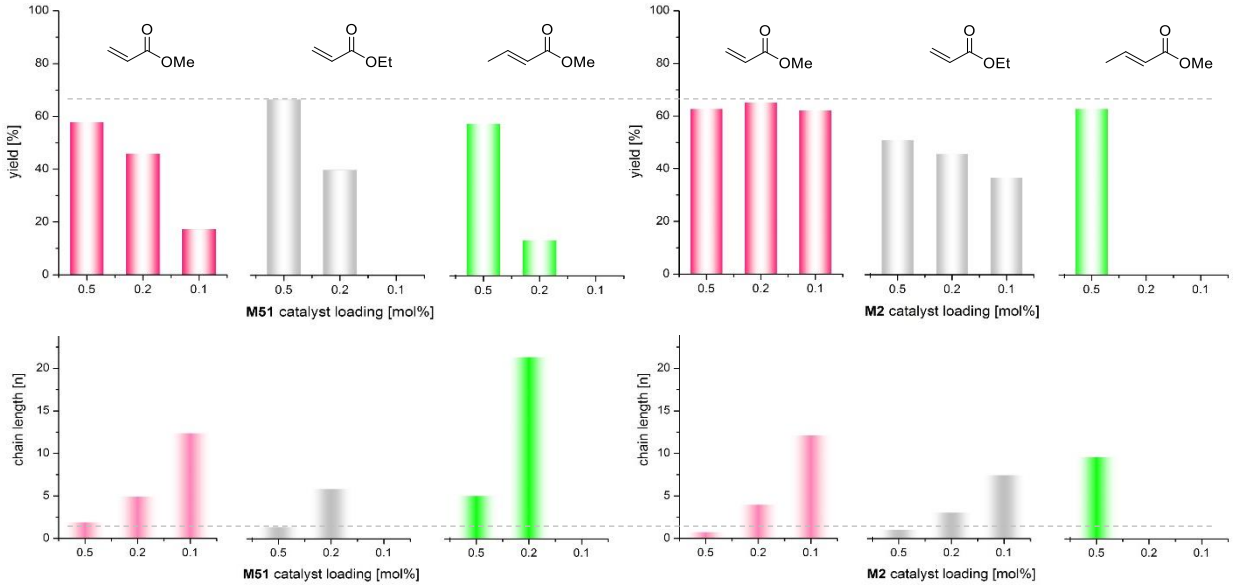

Figure 18: yield and chain length of the product using different reactants and catalysts at different loadings

A comparison with data from literature,[42] recorded using catalyst **M51** and ethyl acrylate, shows the improved degradation by using pre-degraded polyisopren (Table 3). Though a correlation between catalyst-loading and chain length was already drawn, the reported absolute values are throughout bigger than the here presented ones, especially at lower catalyst-loadings while at the same time giving comparable yields.

Table 3: comparison of determined chain lengths to literature values

Catalyst-loading M51 [mol%]	Literature[42]		Determined	
	Chain length [1]	Yield [%]	Chain length [1]	Yield [%]
1.0	1.6	80	n.d	n.d
0.5	3.2	69	1.4	67
0.2	15	<50	5.9	40

The, compared to ethyl acrylate, lower yields reported for methyl acrylate can be reproduced in the case of high catalyst-loadings of 0.5 mol% but in contrast to ethyl acrylate, no rapid decrease occurs at lower catalyst-loadings.

3.5 Mechanistic limitations of the investigated cross-metathesis reaction

As in many other cases, also the here investigated CM reaction does not give all the theoretically possible CM products. Figure 19 shows all the possible outcomes of the CM reaction with methyl acrylate, representative for all CM reactions with polyisoprene presented here as none of those show any significant difference in the structure and composition of the raw product mixture. Of those products only **A**, **B** and **F** can be found, while **C**, **D**, **E**, **G** and **H** cannot be detected in the product mixture. This means, that some reaction pathways are impossible or at least hindered in cases where only minor amounts of that product can be found.

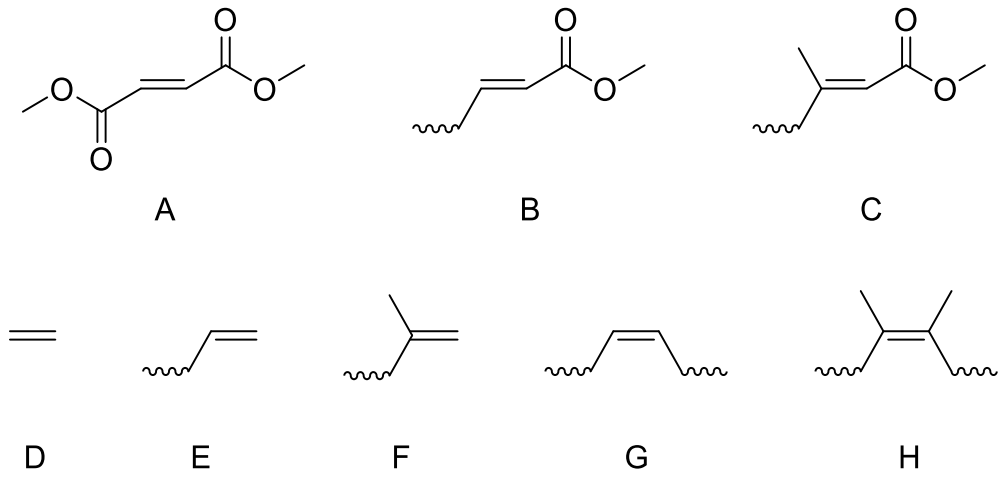

Figure 19: possible CM products

A similar degradation reaction is performed using squalene, giving clearly distinguishable mono- and disubstituted products. Product peaks of comparable disubstituted oligomers cannot be found in MALDI-TOF, proving that **H** is not formed in the degradation of NR. The

lack of **H** can be explained by steric reasons, as two disubstituted carbon atoms need to get in vicinity to each other. This is also valid for the formation of **C** where the carbon atom, although only mono-substituted, bears a huge carboxy group.

It was already shown, that the reaction forming **H** does not occur in metathetic degradation of polyisoprene, while non- or mono-substituted partners such as methylidene or *n*-alkylidenes from other repeating-units form products.[8,46] This non-productive, degenerate pathway occurs here as a side reaction, forming relatively low amounts of cyclic oligomers and shorter chains in the range of 3-16% of the total polyisoprene used.

The other degenerate metathesis, repeatedly reforming methyl acrylate, does not dominate which can be proven by lowering the excess from 5 to 2 eq. of reactant. This does not result in significant changes in chain length and yield, showing not the increased performance one would expect in case of a prevailing non-productive pathway. The same holds true for the non-productive formation of **A** which occurs in the range of 25 to 75% relative to the amount of product molecules. With respect to the used 5-fold excess, those values are much lower than can be expected from a prevailing reaction. The absolute amount of the side-product decreases with the catalyst-loading.

D must be formed during self-metathesis of methyl acrylate, but as it is very volatile, it is lost during work-up and therefore cannot be detected.

G is most likely to be formed, although it is not proven, as its shifts in ^{1}H-NMR spectra correspond greatly to those of the polyisoprene repeating unit. Nevertheless, this metathesis product is non-functionalized (**F**) and therefore behaves like a non-degraded polyisoprene chain, getting removed with residual polyisoprene during work-up. By comparing the integrals of the different repeating unit peaks, the possibility of two **G** groups occurring in one product molecule in notable amounts is disproven (Figure 20). In the here presented case, the oligomers have a mean chain length of 6.5 meaning that the integral of the CH_2 groups should be 29.9 and the integral of the CH_3 groups should be 22.4, which is the case.

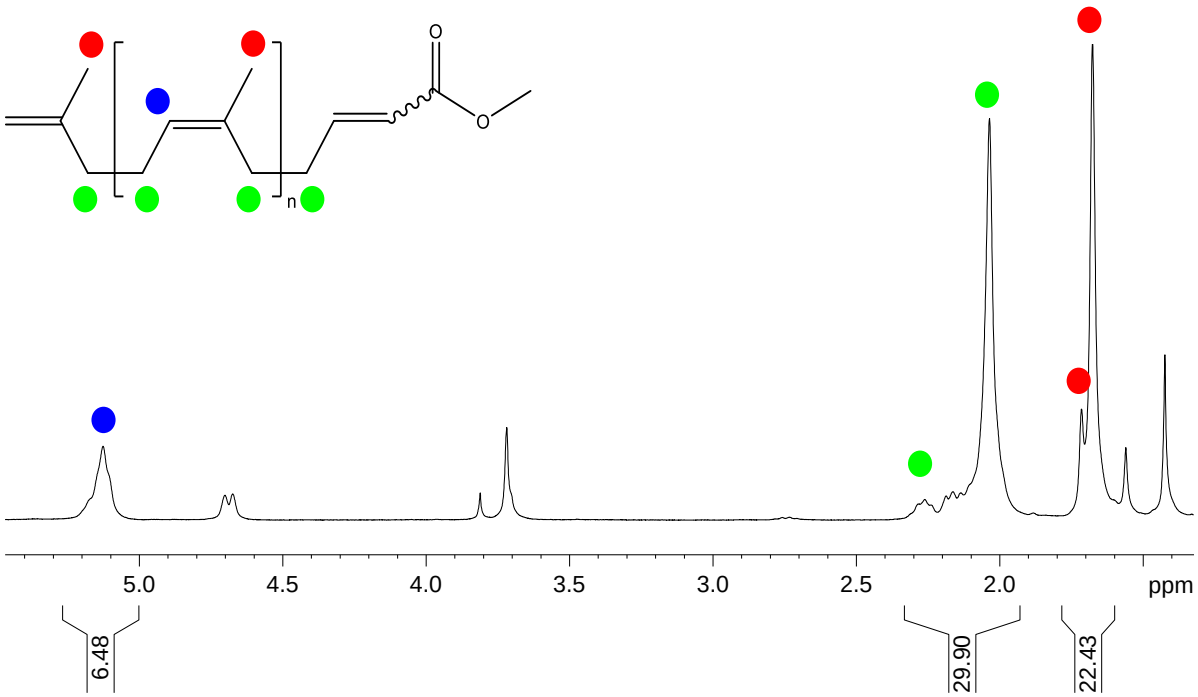

Figure 20: integrals of repeating unit peaks relative to each other (1H-NMR of product from chapter 4.8)

The lack of **G** in the product can be attributed to the relatively short chain length of the products, making the occurrence of two **G** groups very unlikely. Additionally, **G** groups can be expected to be more reactive than the polyisoprene repeating unit due to its lower degree of substitution, leading to a proportionally higher loss of **G** groups.

This is even more expressed in the case of **E** which, aside from **D**, is expected to be the most reactive species formed during the reaction. Nevertheless, it cannot be found in any of the raw products, indicating that due to its high reactivity it is consumed totally by the reaction.

3.6 Summary of the metathetic degradation of polyisoprene with electron-deficient enes

It is shown, that the degradation of polyisoprene via CM with electron-deficient enes can be greatly improved by making the substrate soluble. None of the other measures taken to improve yield and chain-length effects the reaction as much as this pre-degradation step as a product from pre-degraded polyisoprene gives about half the chain-length compared to a product from the degradation of NR-snippets.

It is possible to still gain product at significantly lower catalyst-loadings of down to 0.1 mol% compared to the 0.2 mol% reported in the work this research is based on[42] while retaining the catalyst-loading dependency of the chain-length of the product oligomers, giving reproducible

values down to 0.1 mol%. Lowering the catalyst-loading further to 0.05 mol% shows no product formation in any case.

Although contradicting the catalyst degradation mechanisms described in chapter 2.2, the combination of methyl acrylate and **M2** catalyst gives the highest yield at catalyst-loadings of 0.1 mol%. Aside from that, this formulation gives a mean chain length of 12.1 which is ideal for a source material for water in oil emulsion stabilizers as long chains are more capable of stabilizing than shorter ones. Therefore, this formulation is used from here on for the formation of the HIPE-stabilizer predecessor.

3.7 Functionalization of semi-telechelic natural rubber oligomers

The afore mentioned degradation of polyisoprene with methyl acrylate using the catalyst **M2** is up-scaled by a factor of approximately 20 to get sufficient amounts of stabilizer after functionalization. In contrast to the up until here reported degradation, a shorter than expected chain length of 6.5 at a relatively high yield of 66.5% is observed.

In order to create a suitable surfactant, capable of stabilizing water in oil emulsions, the obtained oligomers need to be functionalized with a polar group. This end-group-functionalization can be performed either at the carboxy group or at the electron-deficient double bond. The functionalization via the Diels-Alder-reaction has already been reported[42] and is therefore not investigated further. Michael-addition of imidazole and amidization with ethanol amine is investigated and shows promising results. Nevertheless, further investigation is necessary.

Another way of functionalization is the saponification with NaOH shown in Figure 21. As carboxylic acid salts are some of the strongest groups in the HLB-concept, a long nonpolar chain is necessary to get the desired HLB-value. This in turn increases greatly the stability of the emulsions the semi-telechelic oligomers are used for and also poorer performing CM degradation reactions, leading to longer chain lengths, gain interest. Additionally, saponification is one of the most straight-forward reactions known, using simple, cheap reactants. Because of this reasons it is the ideal functionalisation for the here presented purpose.

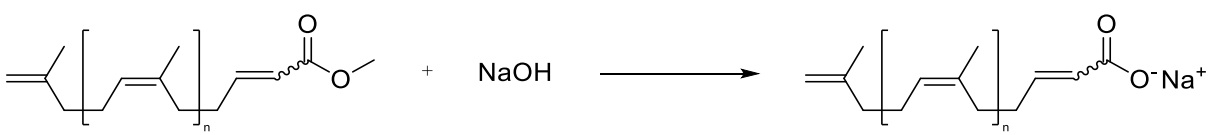

Figure 21: saponification of the ester

The comparison of the ATR-IR spectra of the ester and the salt derived from it clearly shows that the characteristic C=O stretch vibration of the ester at 1728 cm^{-1} is lost and the salts pendant at 1554 cm^{-1} comes up after the reaction while the rest of the spectra stays more or less the same (Figure 22). The band between those two at ~1650 cm^{-1} can be attributed to the stretching vibration of the electron-deficient end-group double bond and does not represent a third carbonyl species.

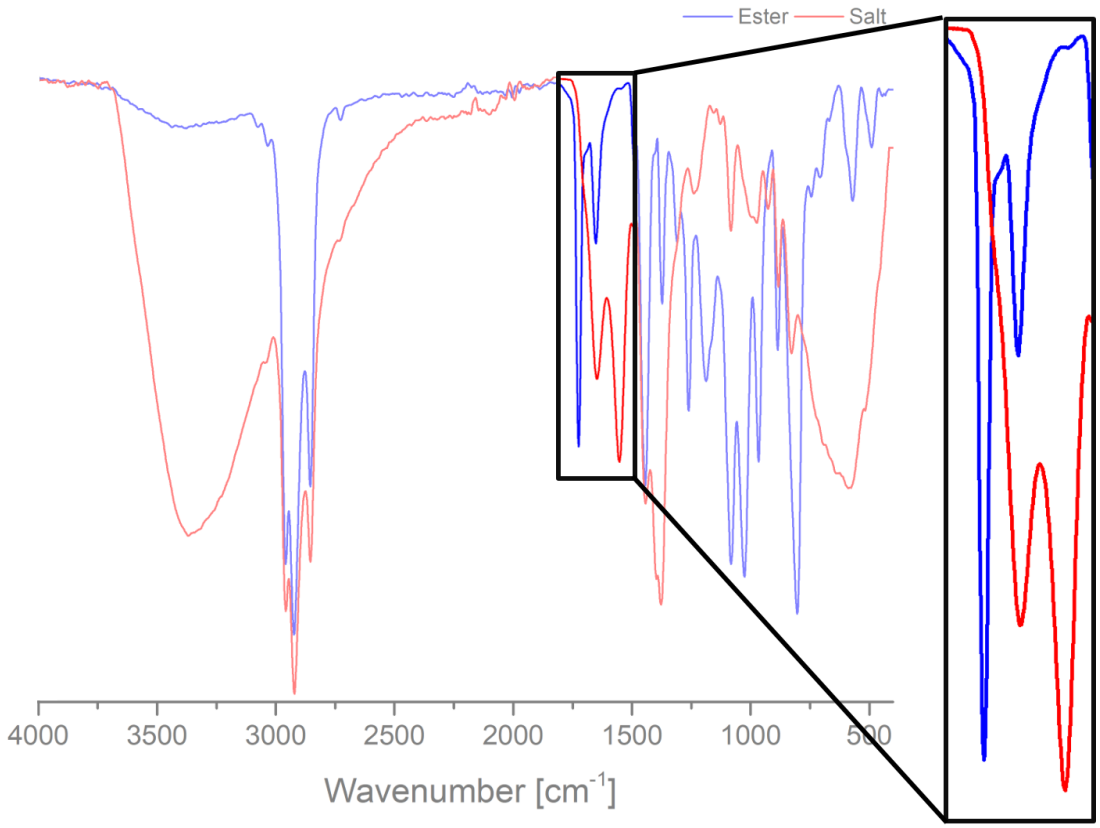

Figure 22: ATR-IR-spectra of the oligomers before and after saponification

Additionally, according to the Bancroft rule, the extraction step, following the reaction, leads to a shift towards higher chain lengths with a higher capability to stabilize the targeted HIPE. Nevertheless, the chain-length determination via ^{1}H-NMR spectroscopy cannot be applied here as the stabilizer is insoluble in D_2O and tends to aggregate, building presumably micelles in $CDCl_3$. This leads to a weakening of signals from inside the micelle, making the integrals of the two different end-groups incomparable and the calculation of the actual chain-length impossible. It is tried to counter this effect by adding trifluoroacetic acid into the NMR-tube in order to protonize the salt. Nevertheless this proves to be ineffective as can be seen in Figure 23.

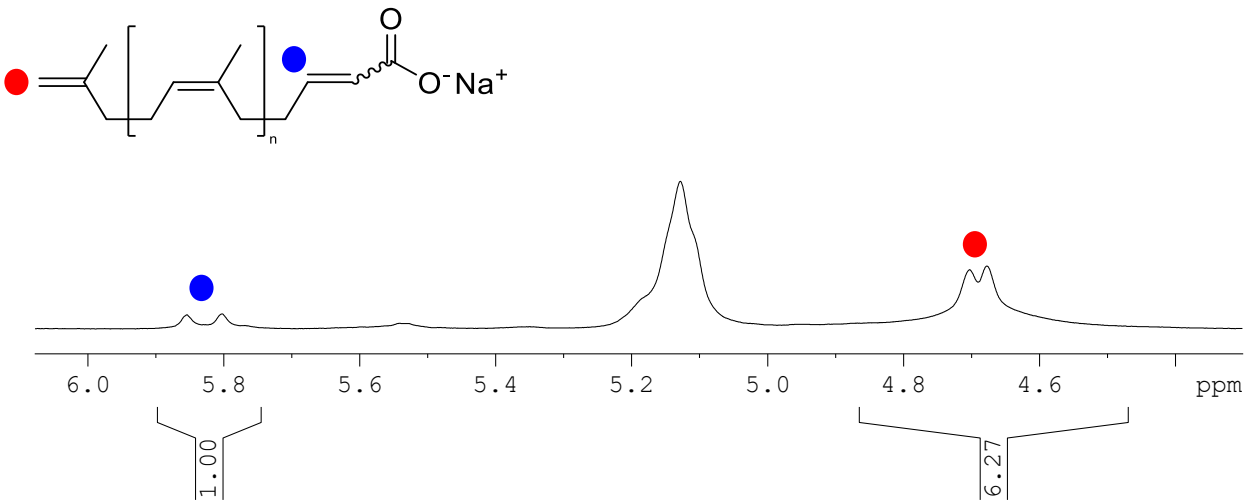

Figure 23: incomparable end-group integrals of the stabilizer

3.8 DCPD-HIPE formation

As the actual chain length of the stabilizer cannot be determined, the HLB is approximated by using the chain length of the ester (6.5), the stabilizer is derived from. This gives a HLB-value of 10.9 which is above the 6, necessary to stabilize a water in oil emulsion. Although it can be expected, that during the extraction step after saponification shorter chains are removed, the yield of 72.3% indicates that the necessary minimal chain length of 9.1, giving a HLB-value of 6, is not reached. Therefore, the addition of NaCl, increasing the polarity of the non-organic phase as well as leading to a densely packed, more stable interphase, is regarded necessary. In order to monitor the stability and possible premature phase separation or loss of structure, the HIPE is investigated under the increased temperature of 80°C it is confronted with when solidified. Figure 24 shows the 20-fold magnification microscope images of the HIPE directly after its formation as well as after 30, 60 and 90 minutes.

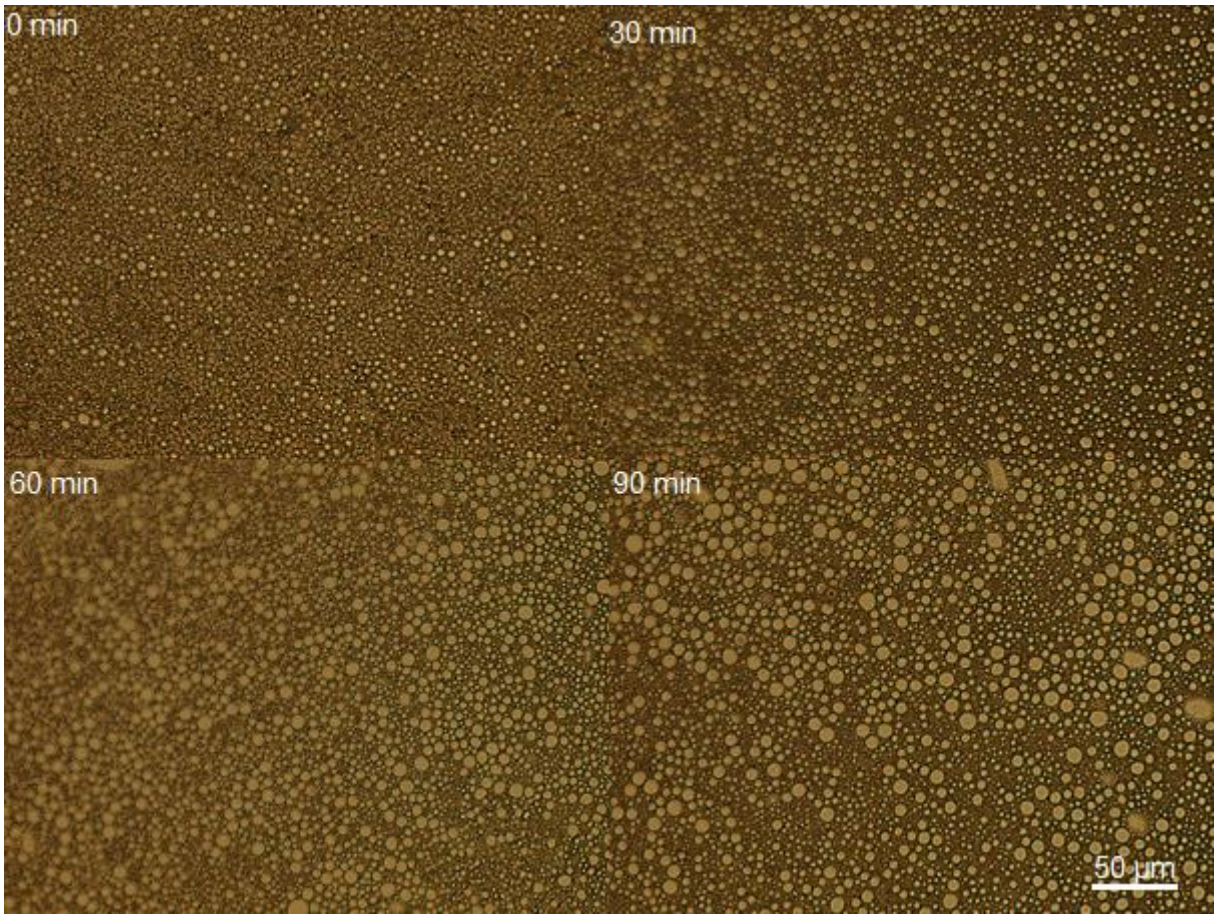

Figure 24: microscope images of HIPE after different times at 80°C

Over this time a slight increase in average bubble size from 8.0 ± 2.1 µm to 12.2 ± 2.6 µm, shown in Figure 25, due to Ostwald ripening is observable while the HIPE structure is maintained. No phase separation can be detected after leaving the HIPE in the drying cabinet for four days. This suggests, that the HIPE is stable enough to freeze its structure during polymerization.

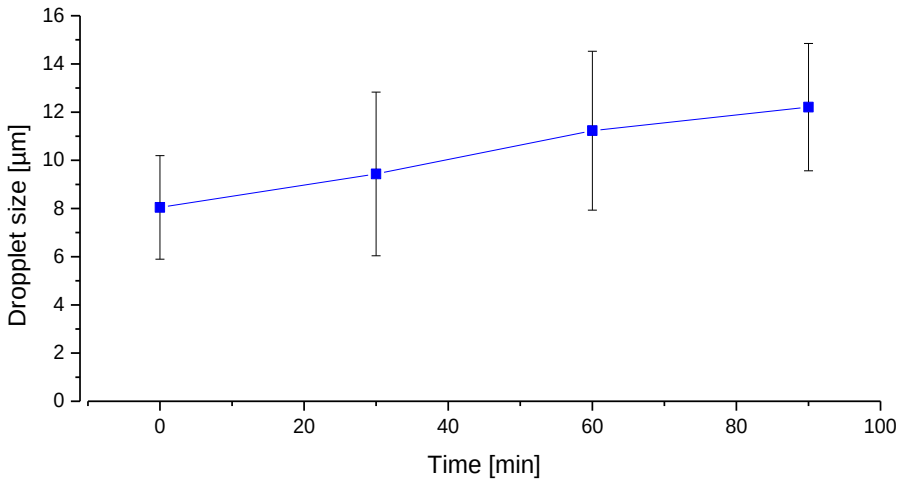

Figure 25: droplet size increase over time at 80°C

3.9 DCPD-polyHIPE

3.6.1 Void and window size

The formed pDCPD-polyHIPE clearly shows a HIPE structure with voids and windows as can be seen in the SEM image of the broken surface of an oxidized monolith sample that can be seen in Figure 26. Oxidation is necessary to make the monolith brittle enough to break it without affecting the structure at the broken surface of the sample. Overall, oxidation is known to not affect the polyHIPEs structure,[47] making it a perfect tool for sample preparation for SEM. The here shown polyHIPE has a mean void size of 8.8 ± 2.1 µm and a window size of 1.8 ± 0.6 µm, showing a droplet size and structure as the HIPE it originates from.

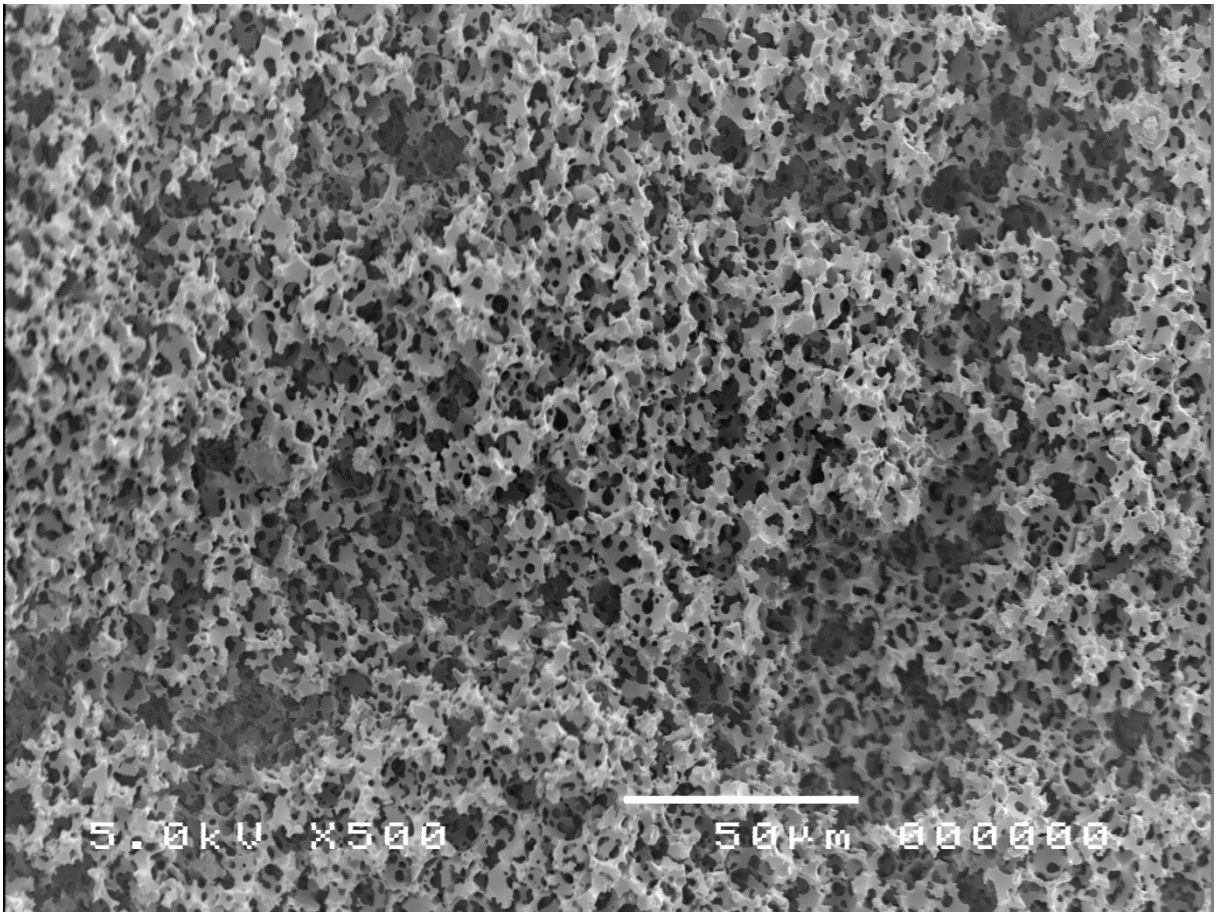

Figure 26: SEM image of the formed DCPD-polyHIPE

3.6.2 Swelling and deswelling behaviour

The swelling and deswelling behaviour is monitored to gain information about the performance of solvents that might be used for possible functionalisation reactions as well as to find possible exploitable features. Figure 27 shows the solvent uptake by swelling and Figure 28 the weight loss relative to the original mass after shrinkage over three swelling/deswelling cycles.

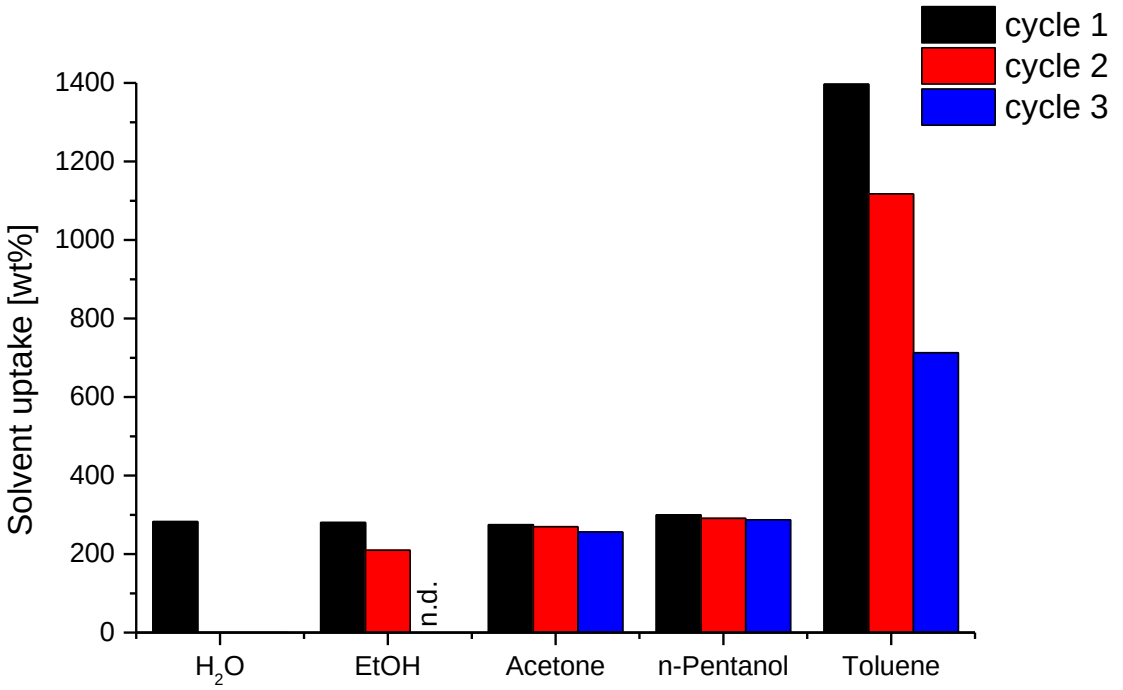

Figure 27: solvent uptake of the polyHIPE disks

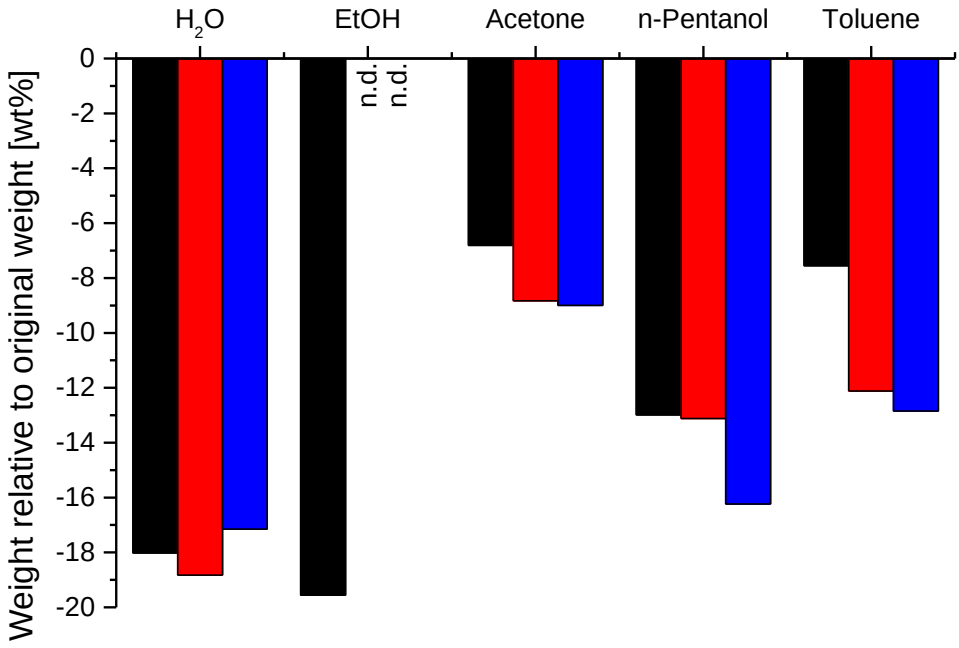

Figure 28: weight of the polyHIPE disks after deswelling relative to the original weight

The disk immersed in toluene shows by far the highest uptake which can be seen in Figure 29 as well as in Figure 30 relative to a disk immersed in water. Due to the very low polarity of toluene, not only the voids are filled, but it is also taken up by the polymer walls. This leads to enlarged voids which are then in turn capable to take up even more toluene.

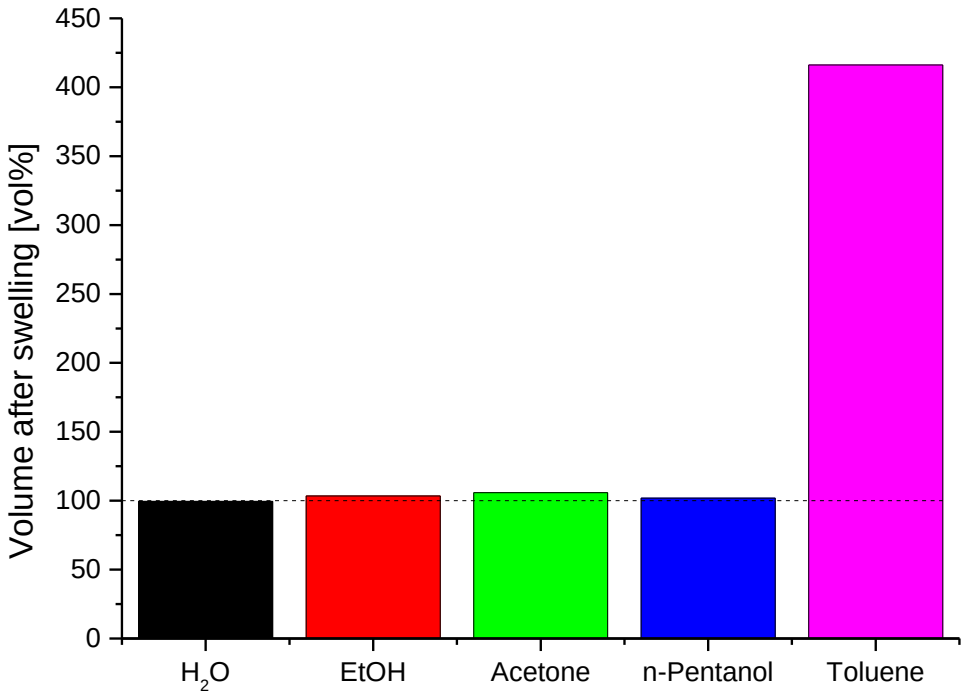

Figure 29: change in volume due to swelling (first swelling)

The decrease in uptake after every deswelling can be explained by the destruction of the polyHIPE-structure that occurs after shrinkage. Figure 31 shows a deformed disk, that is immersed in toluene, after shrinkage.

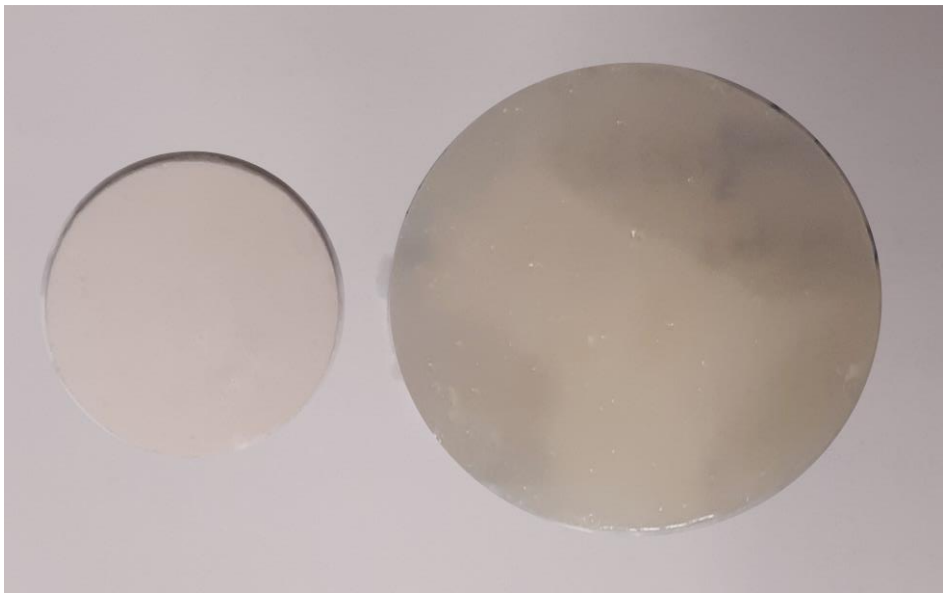

Figure 30: disks swollen with H_2O (left) and toluene (right)

Figure 31: deformed disk deswollen after swelling in toluene

In the case of water, a surprising trend can be observed. While the first swelling process leads to a solvent uptake comparable to that of the less polar solvents, the second and third show no uptake at all. In contrast to the other solvents, the sample disks float at the surface of the water even after forced immersion or applying ultrasound. The samples are then submersed in acetone and in this case, the solvent is taken up again. This behaviourcan be explained by loss of residual stabilizer from the disks,[30] which can be found only in minor amounts in the acetone used for purification after polymerization. Accordingly, during the first swelling, surfactant is still present but during deswelling the surfactant is washed out, leading to a higher repellence between the polar water and the nonpolar polyDCPC walls. The relatively high weight loss after the first deswelling, that exceeds the total amount of stabilizer used, can be explained by residual salt and solvents in the disks as well as to the loss of polymer through damage to the structure by swelling.

Another possible reason for this behaviour is investigated by immersing the disk in NaOH. in order to deprotonate acid groups of residual stabilizer but this can be disproven as this neither leads to any NaOH uptake nor the ATR-IR spectra (Figure 32) show any acid or salt groups of possible residual stabilizer at ~1760 cm^{-1} respectively 1554 cm^{-1}. This also proves, that in fact no more stabilizer can be found in the samples after several immersions and therefore also no covalent incorporation has taken place which can be explained by the lower degree of substitution and the ring-strain of DCPD compared to the non-strained, tri-substituted polyisoprene repeating unit, rendering its attack much less favourable.

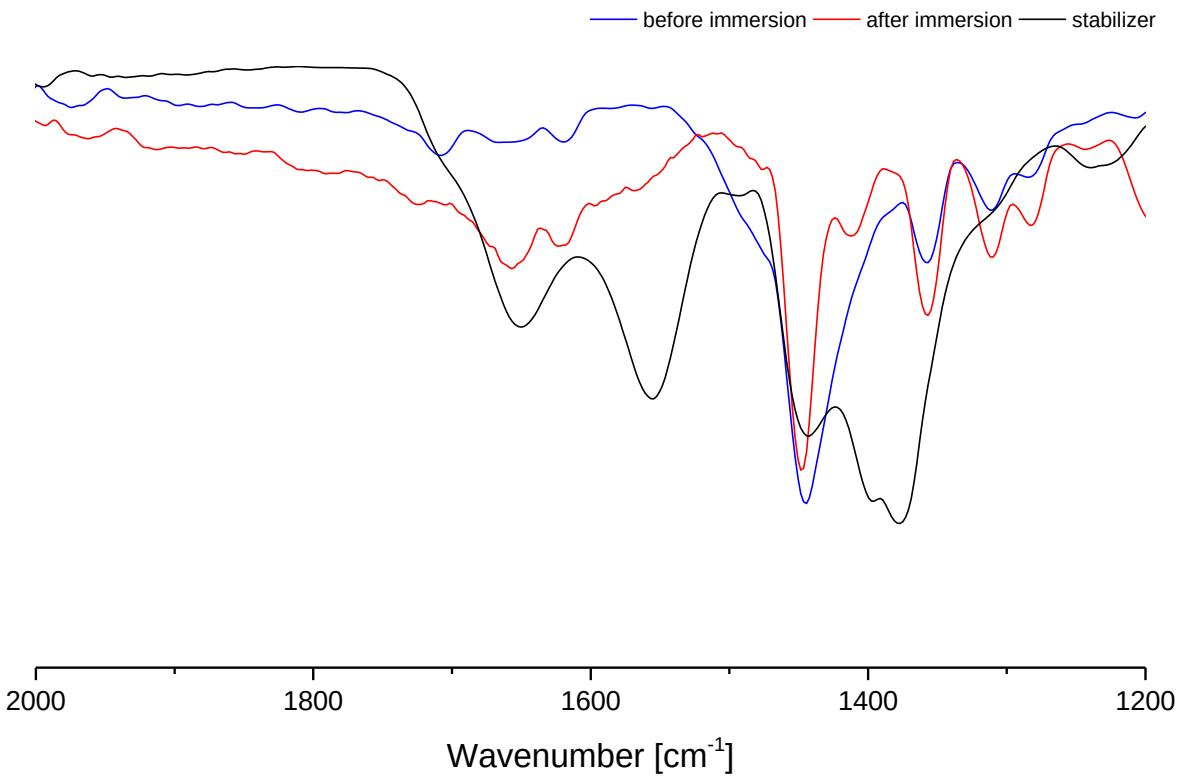

Figure 32: ATR-IR spectra from the surface of a disk before and after immersion in NaOH compared to the used stabilizer

3.6.3 Porosity

The porosity of a polyHIPE depends on the ratio of oil and water in the HIPE it is derived from. By immersing the polyHIPE in a solvent that ideally does not swell but fully fill up all the voids in the sample, the porosity of the sample-disks can be determined, applying Formula 3.[48]

$$porosity = \frac{m_{filled} - m_0}{\rho * V_0} \qquad (3)$$

This gives important information about the uniformity of the samples as it is impossible to investigate the structure as a whole by SEM and larger non-porous domains that can come up during rapid phase separation or imperfections by defective moulding can be formed.

In the here investigated case, the disk immersed in toluene cannot be used due to the massive swelling. The first soaking with water shows a calculated porosity of 62.3% and does not show any swelling at all while the samples slightly swollen by ethanol, acetone and *n*-pentanol, show a mean porosity of 82.0%. This reveals, that water uptake is already hampered in the first swelling attempt as the difference in calculated porosity cannot be explained by the relatively low increase in volume, reaching a maximum value of only 5.9 vol% in the case of acetone.

Therefore, the value of 82.0% represents the porosity of the polyHIPE most accurately, and fits well the targeted 80.0% it should have according to the HIPEs formulation.

3.6.3 Oxidation

Due to the open porosity and the high amount of double bonds, the formed DCPD-polyHIPEs tend to oxidize rapidly under ambient conditions, forming a huge variety of different compounds such as bridging peroxides, carbonyls, hydroxyl groups or hydroperoxy groups.[47,49] This process is visually observable as the white, freshly polymerized polyHIPE turns brown over time (Figure 33).

Figure 33: polyHIPE disk before (left) and after oxidation (right)

The newly formed groups shift the mechanical properties of the polyHIPE to a more brittle behaviour. While a freshly produced sample can be bent and stretched to a certain degree, an oxidized one breaks easily. This can be attributed to increased crosslinking by hydrogen- and peroxide-bridges introduced by the newly formed groups.[49] The oxidation is monitored by ATR-IR spectroscopy at the disk surface and gravimetrically.

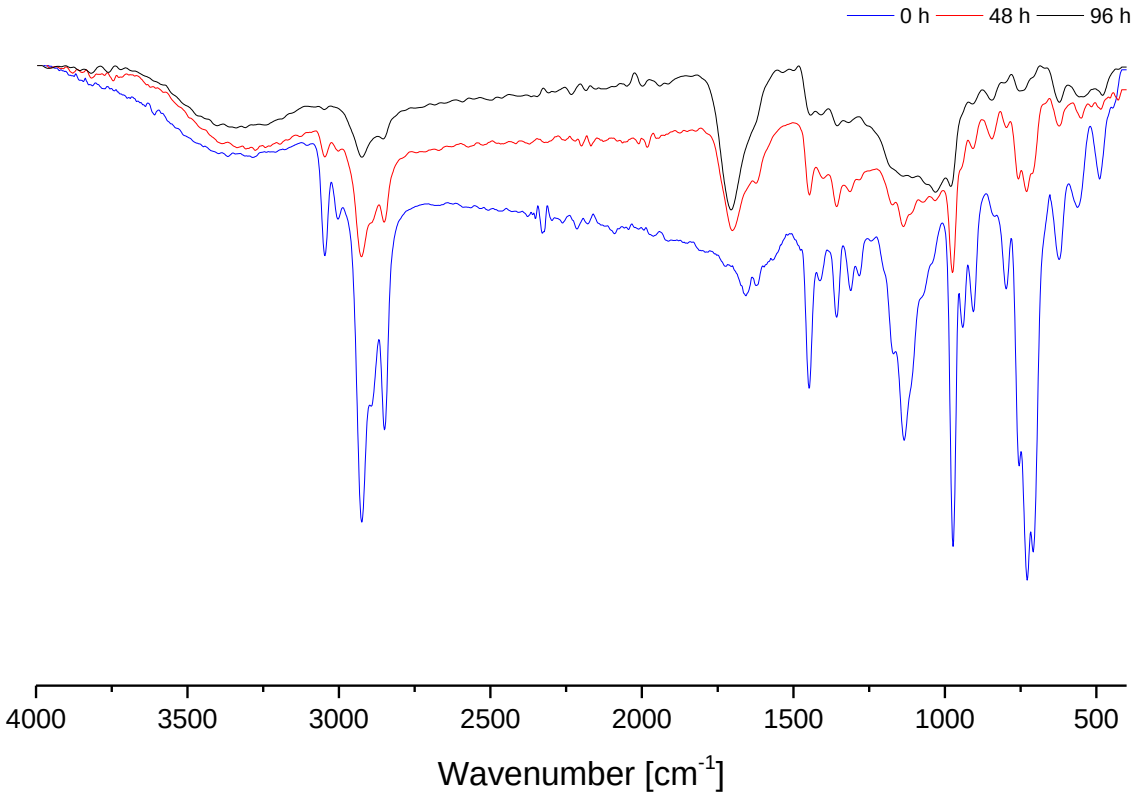

Figure 34: change of ATR-IR spectra from the surface of a polyHIPE disk over time

The spectra shown in Figure 34 leave out those measured after 24 h and 72 h for better visibility due to their similarity to the adjacent ones. It is clearly visible, that the chemical composition of the foams is changed. The upcoming band at 1700 cm^{-1}, representing carbonyl groups, as well as the strongly decreasing absorption of the double bonds at 975 cm^{-1} and 730 cm^{-1} shows the ongoing oxidation.

Figure 35 shows the increase in mass by oxidation, reaching a constant maximum at 37.3%. The sketched line is introduced as a visual aid and does not represent a fit. It can be seen, that the oxidation starts slowly and increases its speed significantly after 24 h. This can be attributed to the autocatalytic nature of the reaction. Here in a first step the double bonds are slowly consumed by autoxidation which leads to the formation of peroxides. Cleavage of these peroxides introduces over time more and more radicals in the system, greatly increasing the speed of oxidation.[50]

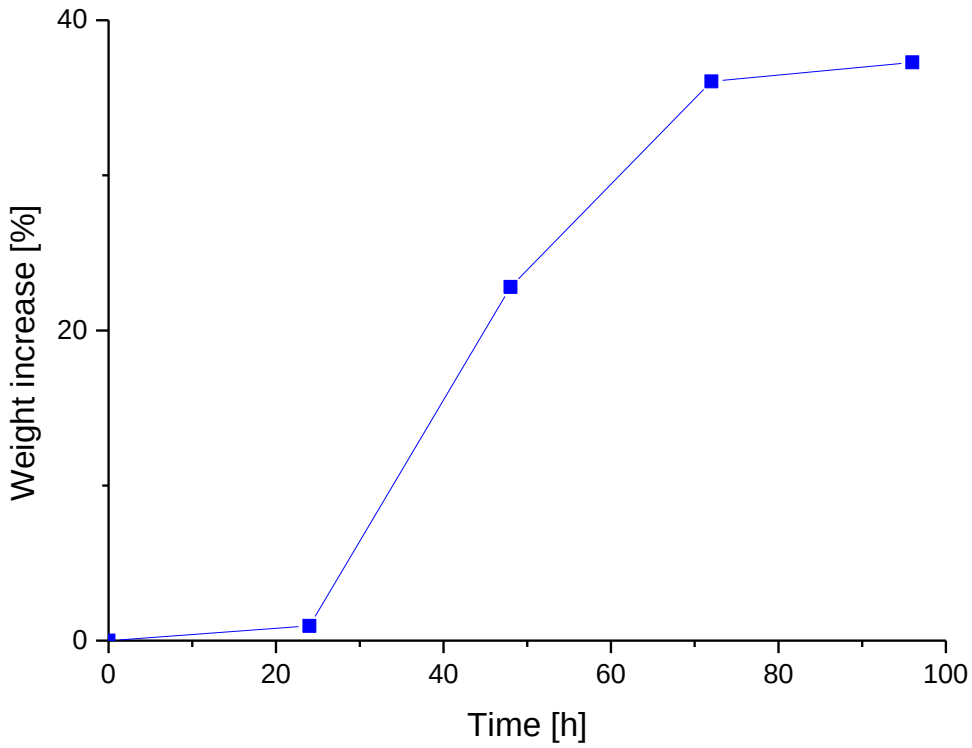

Figure 35: weight increase of the polyHIPE by oxidation

3.10 Summary of the polyHIPE formation

It is shown, that via saponification of semi-telechelic polyisoprene oligomers with ester end-groups a powerful stabilizer for water in oil HIPEs can be formed, at least as long as the respective chain length is not too short. By adding NaCl to the HIPEs formulation, also stabilizers with shorter chain lengths still can form stable emulsions. The formed HIPE, containing 20% DCPD and 80% water, keeps its structure for over 4 days at 80°C and can therefore easily be solidified via ROMP. The resulting porous material has an open cell structure with a void size of here shown polyHIPE has a mean void size of 8.8 ± 2.1 µm and a window size of 1.8 ± 0.6 µm. This polyHIPE shows only mild swelling when immersed into solvents of medium polarity like ethanol, acetone or *n*-pentanol while pronounced swelling in the case of nonpolar toluene and no uptake in the case of polar water is observed. The latter effect is attributed to the removal of the stabilizer by extraction. Via oxidation of the double bonds of the polyHIPE material, a maximal increase in weight of 37.3% can be reached after 96 h.

4 Experimental

4.1 Materials

NR Gloves (Kimberly-Clark Professional KIMTECH* PFE), DCPD (adcr), **M2** ([1,3-Bis(2,4,6-trimethylphenyl)-2-imidazolidinylidene]dichloro(3-phenyl-1H-inden-1ylidene)(tricyclehexyl phosphine)ruthenium(II)), **M51** ([1,3-Bis(2,4,6-trimethylphenyl)-2-imidazolidinylidene] dichloro[[2-(1-methyl-2-oxopropoxy)phenyl]methylene]ruthenium(II)), ethanol (Aldrich), acetone (Aldrich), *n*-pentanol (Fisher Scientific), toluene (Aldrich), dimethyl fumarate (Alfa Aesar), dimethyl maleate (Fluka), maleic acid (Merck), methyl acrylate (TCI chemicals), ethyl acrylate (Aldrich) and methyl crotonate (Aldrich) were used as received.

4.2 Instruments

4.2.1 Chromatography

a) Size exclusion chromatography

SEC chromatographic analysis was performed by Josefine Hobisch on a WGE Dr. Bures SEC3010 with THF as eluent (1 mL/min) and RI-detection.

b) Column chromatography

As stationary phase silica gel 60 from Macherey-Nagel was used in column chromatography together with a hand pump to increase the flow rate.

c) Thin layer chromatography

For TLC analysis in the laboratory TLC silica 60 aluminium plates from Merck without UV-marker were used with a 1% KMnO4-solution in water for spotting.

4.2.2 NMR-Spectroscopy

NMR-spectra were measured on a Bruker Avance 300 MHz equipped with an auto sampler. ^{1}H-NMR spectra were measured at 300.36 MHz and ^{13}C-NMR at 75.53 MHz at a temperature of 25°C. NMR samples were prepared using $CDCl_3$ from Eurisotop. The ^{1}H-NMR spectra were calibrated at the solvent peak at 7.26 ppm respectively 77.16 ppm in the case of ^{13}C-NMR. The relaxation time was set to 5 s in order to grant full relaxation and thereby a more accurate chain length determination.

4.2.3 Mass spectroscopy

Matrix-assisted laser desorption/ionization time-of-flight (MALDI-TOF) mass spectra were recorded on a Waters Micromass MALDI micro MX Time-of-Flight Mass Spectrometer by Karin Bartl. 1,8,9-Anthracenetriol (Dithranol) was used as matrix substance and THF as solvent. Sample solutions were prepared by mixing solutions of Dithranol (10 mg/mL) and the sample (10 mg/mL) in a ratio of 7/2 (v/v). Calibration was done externally with polyethylene glycol standards (5 mg/mL).

4.2.4 Secondary electron microscopy

SEM images were taken with a Jeol JSM-5410 microscope at an acceleration voltage of 5000 V by Prof. Robert Saf. In order to get non-deformed surface, the sample monoliths were oxidized and broken according to 4.12.[47] Before taking the images, they were sputtered with gold at a Biorad Goldcoatingsystem.

4.2.5 Infrared spectroscopy

IR spectra were taken on a ALPHA-P FT-IR Spectrometer from Bruker with an ATR module reflection diamond.

4.2.6 Microscopy

The microscope images were taken on an Olympus BX60 microscope and photographed with an Olympus E-250 camera.

4.2.7 Centrifugation

For centrifugation a HERMLE 323K was used without cooling at a break intensity of 2.

4.2.8 Filtration

Filtration was performed using a Ø4 cm Büchner funnel with MN 85/70 filter paper from Macherey-Nagel. The paper was cut into the Ø4 cm circles and vacuum from a water jet pump was applied during filtration.

4.3 Degradation of squalene with methyl crotonate

366 µL Squalene (1 eq., 765 µmol), 2441 µL (30 eq., 22.92 mmol) methyl crotonate and 5 mL toluene were placed in a 20 mL Schlenk-flask. Alternately vacuum and N_2 flow were applied three times. After bubbling N_2 through the solution for 15 min, the mixture was heated up to 80°C. 3.0 mg (0.6 mol%, 0.46 µmol) of catalyst **M51** were added. The reaction mixture was held at 80°C for 22 h. TLC of the resulting brown raw product (ethyl acetate:cyclohexane 1:15) showed the formation of two different products at R_f = 0.55 and 0.25. The raw product was not purified.

4.4 Metathetic pre-degradation of NR

509.5 mg (1 eq., 7.489 mmol) of NR-snippets were placed in a 50 mL Schlenk-flask together with 25 mL toluene. Alternately vacuum and N_2 flow were applied three times. After bubbling N_2 through the solution for 15 min, the mixture was heated up to 80°C before adding 14.2 mg (0.2 mol%, 15.9 µmol) of catalyst **M2** under N_2 counter flow. As after 24 h only mild degradation was visible, 9.8 mg (0.2 mol%, 14.7 µmol) of catalyst **M51** were added and the temperature was increased to 110°C and held there for another 24 h. The then mostly degraded NR was worked up by filtration and the solvent was removed at the rotary evaporator, giving a dark yellow rubber showing two peaks in SEC.

Yield: 254.0 mg (49.9%, Mn_1 = 14800 g/mol, PDI_1 = 1.9, Mn_2 = 500 g/mol, PDI_2 = 1.7)

ATR-IR: $\tilde{\nu}$ = 2963, 2922, 2848, 1704, 1659, 1450, 1373, 1313, 1239, 1123, 1081, 1036, 1014, 884, 830, 730, 691, 496

4.5 Thermal pre-degradation of natural rubber

18.21 g (267.3 mmol) NR gloves were cut into small pieces (~1 x 1 cm) and placed in a 500 mL round bottom flask 500 mL toluene were added and the closed reaction vessel was stirred at 200 rpm for 48 h with a mechanical stirrer, giving a polyisoprene solution with some suspended particles. The particles were removed by centrifugation at 4000 rpm over 20 min and consequent filtration with filter paper of a pore size of 0.6 µm. Toluene was removed at the rotary evaporator and the product is dried under vacuum.

Yield: 14.17 g (77.8%, M_n = 1300 g/mol, PDI = 2.2)

ATR-IR: $\tilde{\nu}$ = 2961, 2919, 2853, 1712, 1662, 1446, 1373, 1307, 1241, 1126, 1084, 1038, 1012, 887, 834, 729, 692, 502

4.6 Cross-metathesis of natural rubber snippets with ethyl acrylate

211 mg (1 eq., 3.10 mmol) of NR-snippets and 1687 µL (5 eq., 15.50 mmol) ethyl acrylate were placed in a 50 mL Schlenk-flask together with 25 mL toluene. Alternately, vacuum and N_2 flow were applied three times. After bubbling N_2 through the solution for 15 min, the mixture was heated up to 80°C before adding 10.1 mg (0.5 mol%, 15.4 µmol) of catalyst **M51** under N_2 counter flow. The reaction mixture was held at 80°C for 22 h. The volatiles were removed under vacuum and the residual brown sludge was purified via column chromatography (eluent: ethyl acetate:cyclohexane = 1:30, silica: 20 mL). The solvent was removed at the rotary evaporator and the product, a yellow oil, was dried under vacuum.

Yield: 180.1 mg (61.2%, chain length: 2.7)

^{1}H-NMR (300MHz, $CDCl_3$): δ = 6.95 (dt, 0.88H, -C*H*^{trans}=CH-$COOCH_3$); 6.20 (m, 0.12H, -C*H*^{cis}=CH-COO CH_3); 5.82 (d, ^{3}J = 15.7 Hz, 1H, -CH^{trans}=C*H*-COO CH_3 – submersed – CH^{cis}=C*H*-COO CH_3); 5.27-5.02, (m, 2.73H, -C(CH_3)=C*H*-); 4.70, 4.67 (s, 2H, -C(CH_3)=C*H*$_2$); 4.22 (q, 2H, COOC*H*$_2$$CH_3$); 2.40-1.94 (m, 14.9H, -CH2-CH2-); 1.71, 1.68 (s, 11.2H, -C(C*H*$_3$)=CH-, -C(C*H*$_3$)=CH_2); 1.28 (s, 3H, $COOCH_2$C*H*$_3$)

4.7 Cross-metathesis of pre-degraded natural rubber with electron-deficient-enes

This reaction was performed using different catalysts and CM partners. The used amounts and solvents are shown in Table 4.

A stock solution of pre-degraded polyisoprene was prepared (10 mg/mL). 6.2 mL (1 eq, 910 mmol) of this stock solution were placed in a 20 mL Schlenk-flask. 5 eq. of CM partner were added and alternately vacuum and N_2 flow were applied three times. After bubbling N_2 through the solution for 5 min, the mixture was heated up to 80°C. Shortly before the catalyst addition, the catalyst was dissolved in toluene (10 mg/mL). The reaction was held at 80°C for 22 h after adding the catalyst solution under N_2 counter flow. The volatiles were removed under vacuum and the residual brown sludge was purified via column chromatography (eluent: ethyl acetate:cyclohexane = 1:50, silica: 20 mL). The solvent was removed at the rotary evaporator and the product, a yellow oil, was dried under vacuum.

Table 4: amounts of CM partner and catalyst

Reactant	Amount	Amount of catalyst [mg]						Solvent
		M51			M2			
		0.5 mol%	0.2 mol%	0.1 mol%	0.5 mol%	0.2 mol%	0.1 mol%	
Diethyl maleate	571 µL	3.00	-	-	-	-	-	Toluene
Diethyl fumarate	660 mg	3.00	-	-	-	-	-	Toluene
Maleic acid	533 mg	3.00	-	-	-	-	-	THF/ Toluene
Acrylic acid	312 µL	3.00	1.20	-	4.40	1.76	0.88	Toluene
Methyl crotonate	488 µL	3.00	1.20	0.60	4.40	1.76	0.88	Toluene
Methyl acrylate	415 µL	3.00	1.20	0.60	4.40	1.76	0.88	Toluene
Ethyl acrylate	500 µL	3.00	1.20	0.60	4.40	1.76	0.88	Toluene

Product from the degradation with methyl crotonate:

^{1}H-NMR (300MHz, $CDCl_3$): δ = 6.96 (dt, 0.89H, -C*H*^{trans}=CH-$COOCH_3$); 6.21 (m, 0.11H, -C*H*^{cis}=CH-$COOCH_3$); 5.84 (d, ^{3}J = 15.6 Hz, 1H, -CH^{trans}=C*H*-$COOCH_3$ – submersed – -CH^{cis}=C*H*-$COOCH_3$); 5.27-5.01, (m, 5.06H, -C(CH_3)=C*H*-CH_2-, -C(CH_3)=C*H*-CH_3); 3.72 (s, 3H, COOC*H*$_3$); 2.35-1.90 (m, 20.2H, -C*H*$_2$-C*H*$_2$-); 1.68, 1.59, 1.55 (s, 18.2H, -C(C*H*$_3$)=CH-, -C(C*H*$_3$)=CH-C*H*$_3$)

^{13}C{^{1}H}-NMR (75MHz, $CDCl_3$): δ = 167.2 (-*C*$OOCH_3$); 149.4 (-*C*H=CH-$COOCH_3$); 135.9, 135.3, 135.1, 133.8 (-*C*(CH_3)=CH-); 126.3, 125.4, 125.2 (-C(CH_3)=*C*H-); 121.2 (-CH=*C*H-$COOCH_3$); 118.4 (CH_3-*C*H=C(CH_3)-); 51.5 (-COO*C*H_3); 40.1, 40.0 (-*C*H_2-C(CH_3)=CH-CH_3); 32.4, 32.2, 30.9, 30.8, 30.5 (-C(CH_3)=CH-*C*H_2-, -CH=CH-*C*H_2-); 26.5, 26.3, 26.2 (-*C*H_2-C(CH_3)=CH-); 23.6, 23.4 (-C(*C*H_3)=CH-); 15.8 (-C(*C*H_3)=CH-CH_3); 13.5 (*C*H_3-CH=C(CH_3)-)

4.8 Cross-metathesis of pre-degraded natural rubber with methyl acrylate

A stock solution of pre-degraded polyisoprene in toluene was prepared (20 mg/mL). 55 mL (1 eq., 16.1 mmol) of this stock solution were placed in a 100 mL Schlenk-flask. 7.32 mL (5 eq., 80.8 mmol) of methyl acrylate were added, and alternately vacuum and N_2 flow were applied three times. After bubbling N_2 through the solution for 15 min, the mixture was heated up to 80°C. 15.3 mg (0.1 mol%, 16.1 µmol) of catalyst **M2** were dissolved in 1.53 mL toluene shortly before the addition. The reaction was held at 80°C for 22 h after addition of the catalyst solution under N_2 counter flow. The volatiles were removed under vacuum and the residual brown sludge was purified via column chromatography (eluent: ethyl acrylate:cyclohexane =

1:50, silica: 35 mL). The solvent was removed at the rotary evaporator and the product, a yellow oil, was dried under vacuum.

Yield: 855 mg (66.5%, chain length: 6.5)

^{1}H-NMR (300MHz, $CDCl_3$): δ = 6.96 (dt, 0.88H, -C*H*^{trans}=CH-$COOCH_3$); 6.21 (m, 0.12H, -C*H*^{cis}=CH-$COOCH_3$); 5.83 (d, ^{3}J = 15.7 Hz, 1H, -CH^{trans}=C*H*-$COOCH_3$ – submersed – CH^{cis}=C*H*-$COOCH_3$); 5.30-5.00, (m, 6.48H, -C(CH_3)=C*H*-); 4.70, 4.68 (s, 2H, -C(CH_3)=C*H*$_2$); 3.72 (s, 3H, COOC*H*$_3$); 2.34-1.92 (m, 30.1H, -C*H*$_2$-C*H*$_2$-); 1.72, 1.68 (s, 22.4H, -C(C*H*$_3$)=CH-, -C(C*H*$_3$)=CH_2)

^{13}C{^{1}H}-NMR (75MHz, $CDCl_3$): δ = 167.1 (-*C*OOCH_3); 149.2 (-*C*H=CH-$COOCH_3$); 146.0, 145.7 (-*C*(CH_3)=CH_2); 135.3, 135.1, 133.8 (-*C*(CH_3)=CH-); 126.3, 126.1, 125.4, 125.2, 125.0 (-C(CH_3)=*C*H-); 121.2 (-CH=*C*H-$COOCH_3$); 110.1, 109.9 (-C(CH_3)=*C*H_2); 51.5 (-COO*C*H_3); 38.2, 38.1 (-*C*H_2-C(CH_3)=CH_2); 32.4, 32.2, 32.1, 31.0, 30.9, 30.8, 30.5 (-C(CH_3)=CH-*C*H_2-, -CH=CH-*C*H_2-); 26.5, 26.3, 26.2 (-*C*H_2-C(CH_3)=CH-); 23.5, 23.4, 22.6 (-C(*C*H_3)=CH-, -C(*C*H_3)=CH_2)

ATR-IR: $\tilde{\nu}$ = 3380, 2958, 2921, 2854, 1728, 1655, 1491, 1443, 1372, 1309, 1259, 1186, 1082, 1026, 965, 886, 803, 745, 708, 667, 570, 490

4.9 Saponification of semi-telechelic polyisoprene oligomers

855 mg (1 eq., 1.44 mmol) of the CM product from 4.8 were dissolved in 150 mL of ethanol and placed in a 250 mL round bottom flask. 4 mL (53.1 eq., 76.5 mmol) NaOH 50% were added and the mixture was heated up to 75°C and turned brown. After 4 h the solvent was removed with a rotary evaporator. 100 mL of cyclohexane were added and the solution was extracted with 100 mL of water. The nonpolar phase was dried with Na_2SO_4 which was consecutively removed by filtration. The solvent was then removed with a rotary evaporator and the product is dried under vacuum.

Yield: 760 mg (72.3%, chain length: 8.4)

A drop of trifluoroacetic acid was added to the solution in the NMR tube to prevent the formation of micelles and consequent suppression of signals.

^{1}H-NMR (300MHz, $CDCl_3$): δ = 7.06 (dt, 1.07H, -C*H*^{trans}=CH-$COOCH_3$); 6.34 (m, 0.44H, -C*H*^{cis}=CH-$COOCH_3$); 5.83 (d, ^{3}J = 15.5 Hz, 1H, -CH^{trans}=C*H*-$COOCH_3$ – submersed – CH^{cis}=C*H*-$COOCH_3$); 5.30-5.00, (m, 8.72H, -C(CH_3)=C*H*-); 4.70, 4.68 (s, 6.27H, -C(CH_3)=C*H*$_2$); 2.41-1.92 (m, 42.0H, -CH2-CH2-); 1.72, 1.68 (s, 29.2H, -C(C*H*$_3$)=CH-, -C(C*H*$_3$)=CH_2)

$^{13}C\{^{1}H\}$-NMR (75MHz, $CDCl_3$): δ = 171.6 (-*C*OOH); 151.9 (-*C*H=CH-COOH); 146.0 (-*C*(CH_3)=CH_2); 135.3, 135.0, 133.5 (-*C*(CH_3)=CH-); 126.4, 125.4, 125.2, 125.0 (-C(CH_3)=*C*H-); 120.8 (-CH=*C*H-COOH); 109.9 (-C(CH_3)=*C*H_2); 38.22 (-*C*H_2-C(CH_3)=CH_2); 32.3, 32.1, 31.0, 30.3, 29.8 (-C(CH_3)=CH-*C*H_2-, -CH=CH-*C*H_2-); 26.5, 26.3 (-*C*H_2-C(CH_3)=CH-); 23.5, 23.3, 22.6 (-C(*C*H_3)=CH-, -C(*C*H_3)=CH_2)

ATR-IR: $\tilde{\nu}$ = 3368, 2958, 2921, 2854, 1648, 1554, 1493, 1444, 1377, 1307, 1238, 1083, 996, 975, 926, 883, 826, 728, 694, 671, 641, 583, 516

4.10 polyDCPD-HIPE formation

700 mg (1 eq., 1.04 mmol) of stabilizer (product from 4.9), 9.84 g (71.5 eq., 74.4 mmol) DCPD and 100 µL toluene were placed in a 250 mL three necked flask and a homogenous solution was formed under stirring with a mechanical stirrer. 600 mg (9.90 eq., 10.3 mmol) NaCl, dissolved in 40 mL of water, were added dropwise. The resulting white, viscous emulsion was stirred for 1 h at 400 rpm before adding 4.7 mg (66.7 ppm, 5.0 µmol) of **M2** dissolved in 200 µL of toluene. After the initiator was distributed evenly, giving a slightly pink emulsion, the mass was poured into Teflon moulds (Ø30 mm x 2 mm) and placed in the drying cabinet at 80°C for 3 h. The resulting white, solid monoliths were then submersed in acetone for 15 min and dried at room temperature.

ATR-IR: $\tilde{\nu}$ = 3046, 3001, 2926, 2849, 2326, 1656, 1621, 1449, 1411, 1360, 1312, 1280, 1136, 971, 942, 904, 799, 754, 729, 706, 623, 562, 489

4.11 Swelling/deswelling of polyHIPE disks

Disks of a height of 2 mm and diameter of 30 mm were prepared according to 4.10. Five solvents of different polarities, namely water (ε = 80), ethanol (ε = 25), acetone (ε = 21), *n*-pentanol (ε = 15) and toluene (ε = 2.4)[51] were placed in a different beaker each. The disks were immersed into the solvents for 24 h for swelling. The swollen disks were then placed in acetone for 15 min and left to dry for 24 h for deswelling. The swelling and deswelling was performed three times for every disk and their weight and dimensions were recorded for each step.

4.12 Oxidation of polyHIPE

A disk of a height of 2 mm and diameter of 30 mm and a prismatic monolith were prepared according to chapter 4.10. They were placed in the drying cabinet at 40°C for 5 days. The disk

was weighed and an ATR-IR spectrum was measured every 24 h while the monolith was broken in half after the 5th day and a SEM image of the broken surface was taken (Figure 26).

4.13 Void-, window- and bubble-size evaluation

In order to monitor the HIPEs stability and to fully characterize the polyHIPE, the void-, window- and bubble-sizes were measured. Therefore, in case of the HIPE, microscope images and in the case of the polyHIPE, SEM images were taken. At least five different images were used for every generated value and at least one hundred measurements were taken per sample.

List of figures

List of tables

Bibliography

(1) Saiwari, S.; Yusoh, B.; Thitithammawong, A. Recycled Rubber from Waste of Natural Rubber Gloves Blending with Polypropylene for Preparation of Thermoplastic Vulcanizates Compatibilized by Maleic Anhydride. *J. Polym. Environ.* **2019**, *27* (5), 1141–1149. https://doi.org/10.1007/s10924-019-01413-2.

(2) Jana, G. K.; Das, C. K. Recycling Natural Rubber Vulcanizates through Mechanochemical Devulcanization. *Macromol. Res.* **2005**, *13* (1), 30–38. https://doi.org/10.1007/BF03219012.

(3) Tsuchii, A. Microbial Degradation of Natural Rubber. In *Biotransformations*; Singh, V. P. B. T.-P. in I. M., Ed.; Elsevier, 1995; Vol. 32, pp 177–187. https://doi.org/10.1016/S0079-6352(06)80032-9.

(4) Tsuchii, A.; Takeda, K.; Tokiwa, Y. Degradation of the Rubber in Truck Tires by a Strain of Nocardia. *Biodegradation* **1996**, *7* (5), 405–413. https://doi.org/10.1007/BF00056424.

(5) Nawong, C.; Umsakul, K.; Sermwittayawong, N. Rubber Gloves Biodegradation by a Consortium, Mixed Culture and Pure Culture Isolated from Soil Samples. *Brazilian J. Microbiol.* **2018**, *49* (3), 481–488. https://doi.org/10.1016/j.bjm.2017.07.006.

(6) Foxley, G. H. Degradation of Rubber by Chemical Agents in Solution. *Rubber Chem. Technol.* **1961**, *34* (4), 1212–1219. https://doi.org/10.5254/1.3540281.

(7) Wagener, K. B.; Puts, R. D. Acyclic Diene Metathesis Depolymerization of Elastomers. *Am. Chem. Soc. Polym. Prepr. Div. Polym. Chem.* **1991**, *32* (1), 379–380. https://doi.org/10.1002/marc.1991.030120708.

(8) Leimgruber, S.; Trimmel, G. Olefin Metathesis Meets Rubber Chemistry and Technology. *Monatshefte fur Chemie* **2015**, *146* (7), 1081–1097. https://doi.org/10.1007/s00706-015-1501-0.

(9) Banks, R. L.; Bailey, G. C. Olefin Disproportionation. *Ind. Eng. Chem. Prod. Res. Dev.* **1964**, *3* (3), 170–173. https://doi.org/10.1021/i360011a002.

(10) Astruc, D. The Metathesis Reactions: From a Historical Perspective to Recent Developments. *New J. Chem.* **2005**, *29* (1), 42–56. https://doi.org/10.1039/B412198H.

(11) Chatterjee, A. K.; Choi, T.-L.; Sanders, D. P.; Grubbs, R. H. A General Model for Selectivity in Olefin Cross Metathesis. *J. Am. Chem. Soc.* **2003**, *125* (37), 11360–11370. https://doi.org/10.1021/ja0214882.

(12) Jean-Louis Hérisson, P.; Chauvin, Y. Catalyse de Transformation Des Oléfines Par Les

Complexes Du Tungstène. II. Télomérisation Des Oléfines Cycliques En Présence d'oléfines Acycliques. *Die Makromol. Chemie* **1971**, *141* (1), 161–176. https://doi.org/10.1002/macp.1971.021410112.

(13) Grubbs, R. H. *Handbook of Metathesis*, 1st ed.; WILEY-VCH: Weinheim, 2003. https://doi.org/10.1002/9783527619481.

(14) Ledoux, N. Ruthenium Olefin Metathesis Catalysts : Tuning of the Ligand Environment. PhD. Dissertation, Universiteit Gent, 2007.

(15) Schrock, R. R. J.; Murdzek, J. S.; Bazan, G. C.; Robbins, J.; DiMare, M.; O'Regan, M. Synthesis of Molybdenum Imido Alkylidene Complexes and Some Reactions Involving Acyclic Olefins. J. Am. Chem. Soc. 1990, 112, 3875–3886.), 3875–3886. https://doi.org/10.1021/ja00166a023.

(16) Schwab, P.; Grubbs, R. H.; Ziller, J. W. Synthesis and Applications of RuCl2(Cover CHR')(PR3)2: The Influence of the Alkylidene Moiety on Metathesis Activity. *J. Am. Chem. Soc.* **1996**, *118*, 100–110. https://doi.org/10.1021/ja952676d.

(17) Scholl, M.; Ding, S.; Lee, C. W.; Grubbs, R. H. Synthesis and Activity of a New Generation of Ruthenium-Based Olefin Metathesis Catalyst Coordinated with 1,3-Dimesityl-4,5-Dihydroimidazol-2-Ylidene Ligands. *Org. Lett.* **1999**, *1*, 953–956. https://doi.org/10.1021/ol990909q.

(18) Sanford, M. S.; Love, J. A.; Grubbs, R. H. A Versatile Precursor for the Synthesis of New Ruthenium Olefin Metathesis Catalysts. *Organometallics* **2001**, *20* (25), 5314–5318. https://doi.org/10.1021/om010599r.

(19) Harrity, J. P. A.; Visser, M. S.; Gleason, J. D.; Hoveyda, A. H. Ru-Catalyzed Rearrangement of Styrenyl Ethers. Enantioselective Synthesis of Chromenes through Zr- and Ru-Catalyzed Processes. *J. Am. Chem. Soc.* **1997**, *119*, 1488–1489. https://doi.org/10.1021/ja9636597.

(20) Kingsbury, J. S.; Hoveyda, A. H. Regarding the Mechanism of Olefin Metathesis with Sol−Gel-Supported Ru-Based Complexes Bearing a Bidentate Carbene Ligand. Spectroscopic Evidence for Return of the Propagating Ru Carbene. *J. Am. Chem. Soc.* **2005**, *127* (12), 4510–4517. https://doi.org/10.1021/ja042668+.

(21) Dinger, M. B.; Mol, J. C. Degradation of the Second-Generation Grubbs Metathesis Catalyst with Primary Alcohols and Oxygen - Isomerization and Hydrogenation Activities of Monocarbonyl Complexes. *Eur. J. Inorg. Chem.* **2003**, No. 15, 2827–2833. https://doi.org/10.1002/ejic.200200702.

(22) Soon, H. H.; Wenzel, A. G.; Salguero, T. T.; Day, M. W.; Grubbs, R. H. Decomposition of Ruthenium Olefin Metathesis Catalysts. *J. Am. Chem. Soc.* **2007**, *129* (25), 7961–7968. https://doi.org/10.1021/ja0713577.

(23) Bailey, G. A.; Fogg, D. E. Acrylate Metathesis via the Second-Generation Grubbs Catalyst: Unexpected Pathways Enabled by a PCy3-Generated Enolate. *J. Am. Chem. Soc.* **2015**, *137* (23), 7318–7321. https://doi.org/10.1021/jacs.5b04524.

(24) Santos, A. G.; Bailey, G. A.; Dos Santos, E. N.; Fogg, D. E. Overcoming Catalyst Decomposition in Acrylate Metathesis: Polyphenol Resins as Enabling Agents for PCy 3 -Stabilized Metathesis Catalysts. *ACS Catal.* **2017**, *7* (5), 3181–3189. https://doi.org/10.1021/acscatal.6b03557.

(25) Ferreira, L. A.; Schrekker, H. S. Augmentation of Productivity in Olefin Cross-Metathesis: Maleic Acid Does the Trick! *Catal. Sci. Technol.* **2016**, *6* (22), 8138–8147. https://doi.org/10.1039/c6cy01181k.

(26) Atlas Powder Company. *Atlas Surface Active Agents*, 1st ed.; Wilmington, 1948.

(27) Griffin, W. C. Classification of Surface-Active Agents by “HLB.” *J. Soc. Cosmet. Chem.* **1949**, *1*, 311–326. https://doi.org/10.1155/2012/187421.

(28) Davies, J. T. A Quantitative Kinetic Theory of Emulsion Type. i. Physical Chemistry of the Emulsifying Agent. In *Proc. 2nd Int. Congr. Surface Activity*; London, 1957; pp 426–438.

(29) Bancroft, W. D. The Theory of Emulsification. *J. Phys. Chem.* **1913**, *17* (6), 501–519. https://doi.org/10.1021/ja01665a002.

(30) Cameron, N. R.; Krajnc, P.; Silverstein, M. S. Colloidal Templating. In *Porous Polymers*; 2011; pp 119–172. https://doi.org/10.1002/9780470929445.ch4.

(31) Cameron, N. R. High Internal Phase Emulsion Templating as a Route to Well-Defined Porous Polymers. *Polymer (Guildf).* **2005**, *46* (5), 1439–1449. https://doi.org/10.1016/j.polymer.2004.11.097.

(32) Lissant, K. J. Process of Cleaning Wells with Carbon. US 3732166, 1973. https://doi.org/10.1111/j.1559-3584.1927.tb04229.x.

(33) Lissant, K. J. Method of Transporting Bulksolids. US 3617095, 1971. https://doi.org/10.1016/0375-6505(85)90011-2.

(34) Lissant, J. K. Process of Cleaning Piping Systems. US 3523826, 1970. https://doi.org/10.1111/j.1559-3584.1927.tb04229.x.

(35) Lissant, K. J.; Waddell, P. E. E.; Hyman, F. Use of Emulsions in Crowd Control. US3983213, 1976.

(36) Rajagopalan, V.; Solans, C.; Kunieda, H. ESR Study on the Stability of W/O Gel-Emulsions. *Colloid Polym. Sci.* **1994**, *272* (9), 1166–1173. https://doi.org/10.1007/BF00652387.

(37) Kizling, J.; Kronberg, B. On the Formation and Stability of Concentrated Water-in-Oil Emuslions, Aphrons. *Colloids and Surfaces* **1990**, *50*, 131–140. https://doi.org/10.1016/0166-6622(90)80258-6.

(38) Chen, H. H.; Ruckenstein, E. Correlation between the Stability of Concentrated Emulsions and the Interfacial Free Energy between the Two Phases. *J. Colloid Interface Sci.* **1990**, *138* (2), 473–479. https://doi.org/10.1016/0021-9797(90)90229-H.

(39) Lissant, K. J.; Peace, B. W.; Wu, S. H.; Mayhan, K. G. Structure of High-Internal-Phase-Ratio Emulsions. *J. Colloid Interface Sci.* **1974**, *47* (2), 416–423. https://doi.org/10.1016/0021-9797(74)90273-2.

(40) S. Silverstein, M. PolyHIPEs: Recent Advances in Emulsion-Templated Porous Polymers. *Prog. Polym. Sci.* **2014**, *39*, 199–234. https://doi.org/10.1016/j.progpolymsci.2013.07.003.

(41) Williams, J. M.; Wrobleski, D. A. Spatial Distribution of the Phases in Water-in-Oil Emulsions. Open and Closed Microcellular Foams from Cross-Linked Polystyrene. *Langmuir* **1988**, *4* (3), 656–662. https://doi.org/10.1021/la00081a027.

(42) Abbas, M.; Neubauer, M.; Slugovc, C. Converting Natural Rubber Waste into Ring-Opening Metathesis Polymers with Oligo-1,4-: Cis -Isoprene Sidechains. *Polym. Chem.* **2018**, *9* (14), 1763–1766. https://doi.org/10.1039/c8py00233a.

(43) Madorsky, S. L.; Straus, S.; Thompson, D.; Williamson, L. Pyrolysis of Polyisobutene (Vistanex), Polyisoprene, Polybutadiene, GR-S, and Polyethylene in a High Vacuum. *J. Res. Natl. Bur. Stand. (1934).* **1949**, *42*. https://doi.org/10.1002/pol.1949.120040510.

(44) Umicore Grubbs Catalyst M51 https://pmc.umicore.com/en/products/umicore-grubbs-catalyst-m51/%0A (accessed Jul 20, 2019).

(45) Umicore Grubbs Catalyst M2 https://pmc.umicore.com/en/products/umicore-grubbs-catalyst-m2/%0A (accessed Jul 20, 2019).

(46) Martínez, A.; Gutiérrez, S.; Tlenkopatchev, M. A. Metathesis Transformations of Natural Products: Cross-Metathesis of Natural Rubber and Mandarin Oil by Ru-Alkylidene Catalysts. *Molecules* **2012**, *17* (5), 6001–6010.

https://doi.org/10.3390/molecules17056001.

(47) Kovacic, S.; Jeřábek, K.; Krajnc, P.; Slugovc, C. Ring Opening Metathesis Polymerisation of Emulsion Templated Dicyclopentadiene Giving Open Porous Materials with Excellent Mechanical Properties. *Polym. Chem.* **2012**, *3* (2), 325–328. https://doi.org/10.1039/c2py00518b.

(48) Idris, N. H.; Rahman, M. M.; Wang, J.-Z.; Liu, H.-K. Microporous Gel Polymer Electrolytes for Lithium Rechargeable Battery Application. *J. Power Sources* **2012**, *201*, 294–300. https://doi.org/10.1016/j.jpowsour.2011.10.141.

(49) Kovačič, S.; Preishuber-Pflügl, F.; Slugovc, C. Macroporous Polyolefin Membranes from Dicyclopentadiene High Internal Phase Emulsions: Preparation and Morphology Tuning. *Macromol. Mater. Eng.* **2014**, *299* (7), 843–850. https://doi.org/10.1002/mame.201300400.

(50) Bauman, R. G.; Maron, S. H. Oxidation of Polybutadiene. I. Rate of Oxidation. *J. Polym. Sci.* **1956**, *22* (100), 1–12. https://doi.org/10.1002/pol.1956.1202210001.

(51) Riddick, J. A.; Bunger, W. B.; Sakano, T. K. *Organic Solvents: Physical Properties and Methods of Purification. Fourth Edition*; John Wiley and Sons,New York, NY: United States, 1986.